

**Institute for Particle Physics Phenomenology
Durham University**

M.Sc. thesis in Physics
submitted by

Thimo Preis
born in Hamburg, Germany

handed in on
8th September 2020

A strong-field kinetic perspective on particle production and Higgsproduction from nonequilibrium QFT

This master thesis has been carried out by Thimo Preis at the
Institute for Particle Physics Phenomenology at **Durham University**
under the supervision of
Prof. Valentin Khoze and **Prof. Michael Spannowsky**

A strong-field kinetic perspective on particle production and Higgsproduction from nonequilibrium QFT

Thimo Preis

Abstract

In an effort to compare the nonequilibrium 2PI real-time Schwinger-Keldysh formalism and the asymptotic state construction of vacuum theory, we explore particle production including a strong field in a nonequilibrium kinetic setting. Employing a loop expansion to leading order, we derive a scalar strong-field kinetic system which is complete to leading order $\mathcal{O}(\lambda)$ in a strong-field coupling counting. Together with the 2PI equations of motion for statistical and spectral dynamics under the kinetic limit, a kinetic equation and a background field equation for the collisional strong-field regime is derived. With this self-consistent kinetic system for strong-field dynamics at our disposal, we identify different mechanisms for particle production in kinetic theory. Collisionless particle production arises from a $\mathcal{O}(\lambda^0)$ drift term, where in particular production of gap-less modes becomes possible in the presence of a tachyonic instability. Collisional particle production proceeds through $\mathcal{O}(\lambda)$ inelastic scattering processes. These mechanisms for particle production are driven by fluctuations of the strong background field, where the latter is sub-leading to the former in the strong-field coupling and facilitates particle production in the language of scattering amplitudes and decay rates. Such a description facilitates a comparison to particle production processes in vacuum theory, which we explore on the example of the Higgsproduction mechanism. By virtue of formulating explicit collision terms, we are able to isolate a local dynamical scattering amplitude and a corresponding dynamical decay rate, both are directly dependent on the fluctuations of the strong background field. A translation to scattering expressions of vacuum theory is achieved to remarkable agreement by artificially setting the energy contribution of the background field to zero in order to bridge the otherwise necessary dynamical process of thermalization. By comparison we demonstrate how our strong-field kinetic description generalizes a standard kinetic description of near-equilibrium Bose-Einstein condensation by coupling statistical to off-shell strong-field dynamics.

Contents

1	Introduction and overview	1
1.1	Outline	1
1.2	Comparison of vacuum QFT and nonequilibrium QFT	2
1.3	Overview	7
2	Higgspllosion from the perspective of vacuum QFT	8
2.1	Introduction to Higgspllosion	8
2.2	Characteristic features of Higgspllosion	9
2.3	Spontaneous symmetry breaking and Goldstone's theorem	11
2.4	Broken scalar ϕ^4 theory	12
2.5	The regime of Higgspllosion	13
3	Particle production in nonequilibrium strong-field kinetic theory	15
3.1	Concerning particles	15
3.2	Nonequilibrium quantum field theory for scalar fields	17
3.3	The Goldstone theorem revisited - SSB in NeqQFT	25
3.4	Scalar strong-field kinetic theory	26
3.5	Particle production in strong-field kinetic theory at leading order in the coupling	44
3.6	Conclusion	55
	References	59
4	Acknowledgements	62

1 Introduction and overview

1.1 Outline

This thesis makes an effort to derive a nonequilibrium framework in which one can describe strong-field phenomena and particle production in the kinetic regime. To make contact with particle production in vacuum theory, we explore and compare particle production on the example of the novel Higgspllosion mechanism [1]. Crucially, we do not aim to describe Higgspllosion in a nonequilibrium framework in this work. In contrast, we will elaborate on and derive a framework suitable for describing a wide class of strong-field phenomena. Still, a focus on Higgspllosion as an example for strong-field particle production is kept throughout. To make the reader acquainted with Higgspllosion and its context, we will separately introduce its language and consequences in 2 and reference points of connection in our nonequilibrium formalism as we discuss certain mechanisms of particle production. We stress however that the main focus lies on providing a framework describing scalar strong-field kinetics, on discussing strong-field particle production and on making a connection between vacuum and nonequilibrium theory, such that this thesis can be read independently of its application to Higgspllosion.

If we aim to investigate scalar strong-field phenomena in a nonequilibrium framework, we need to provide a theoretical framework which facilitates a comparison with vacuum theory and encompasses nonequilibrium phenomena at the same time. To this end, we derive a scalar strong-field kinetic system from the first principles of nonequilibrium QFT which directly relates spectral and statistical dynamics to fluctuations of the strong background field. Particle production processes can be driven by strong-field dynamics, where a full account of the dynamics in terms of an established particle picture requires one to employ a strong-field kinetic theory. The underlying comparison between vacuum and nonequilibrium theory then additionally entails understanding the particle picture underlying the two different frameworks. The standard asymptotic state formalism defines particles as free external excitations of the field described by well-defined delta-peaks in the underlying constant spectral function in the asymptotic past and asymptotic future. The 2PI framework facilitates a strong-field kinetic description relying on particles with dynamical and field-dependent delta-shaped spectral functions participating in the dynamics. In the course of this comparison, we will have to translate expressions to conventional descriptions in vacuum theory. Such a translation requires one to track degrees of freedom, since complexity is reduced from nonequilibrium QFT towards vacuum QFT, where the latter neglects dynamics incorporated in the former. One example is the dynamical background field, whose strong fluctuations will facilitate particle production. In the reduction towards vacuum QFT, the background field

thermalizes to a constant late-time vacuum expectation value (VEV). Kinetic theory then facilitates considering the real-time dynamics of an underlying process involving the background field in contrast to the asymptotic framework of vacuum theory. Our strong-field kinetic system will enable one to consider the dynamics of scattering amplitudes and decay rates through a coupled set of equations of motion by providing suitable initial conditions.

In a particular effort towards identifying Higgspllosion in a nonequilibrium framework, the Higgspllosion initial state will not be observable as a particle in a real-time formalism. It describes an intermediate state corresponding to a degree of freedom propagating in the loop for the underlying interaction. The Higgspllosion process will only become apparent upon considering appropriate observables, such as the occupation number for the initial and final particle state. Translating the particle picture facilitated by nonequilibrium kinetic theory to that facilitated by the standard asymptotic state formalism is therefore essential in understanding the additional degrees of freedom contained within the former description to understand Higgspllosion and mechanisms of particle production as derived in the latter.

To this end, let us therefore be precise about the differences for the frameworks employed.

1.2 Comparison of vacuum QFT and nonequilibrium QFT

This thesis aims to approach particle production from the viewpoint of nonequilibrium QFT. By doing so, we have to bridge two different frameworks, namely the perturbative S -matrix formulation of quantum field theory (vQFT) and the real-time Schwinger-Keldysh nonequilibrium treatment of quantum field theory (NeqQFT). We will here discuss and compare what we are implying when talking about these two machineries. Everything we are discussing in this section can be found in conventional textbooks [2, 3].

QFT has proven itself as a universal language for a wide class of phenomena arising in our physical reality. If we have a system where (quantum, thermal, ...) fluctuations and locality (in space, time) describe the system, then it will very likely be described by QFT. Effective descriptions formulated prior to QFT are contained in this framework and can be recovered by enforcing certain sensible special cases, which is depicted in 1.1.

1.2.1 Vacuum QFT

Specializing NeqQFT to the case of thermal equilibrium at zero temperature amounts to the vacuum formalism, treated in many textbooks like [2]. Starting from a Lagrangian

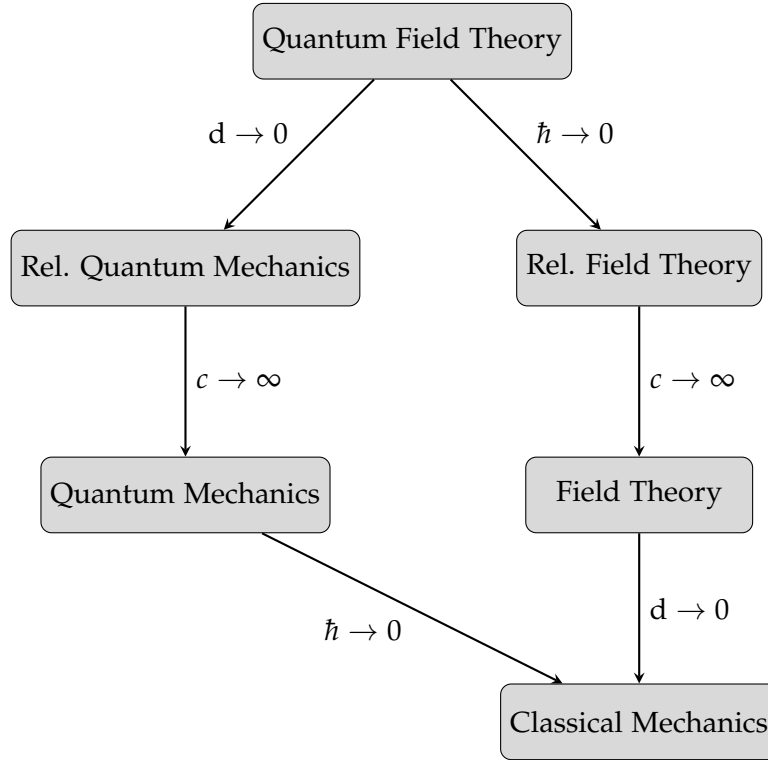


Figure 1.1: The flow of effective descriptions contained in QFT.

\mathcal{L} for the system at hand, one follows a chain of reasoning to arrive at the perturbative, asymptotic state S -matrix formulation of scattering events yielding observables such as decay rates and cross sections.

In order to get a perturbative description for small couplings, one expands around the free theory. This allows one to formulate time-ordered N -point correlators to a given order in the coupling.

One relates the interacting theory to a perturbative free description by translating the interacting vacuum to the free vacuum and resumming the evolution operator via Dyson's formula. The former translation is achieved by virtue of the *adiabatic limit* $t \rightarrow \infty(1 - i\epsilon)$, which can be motivated from the point of view of thermal QFT. It corresponds to a double-scaling limit of asymptotic initial time $t_0 \rightarrow -\infty$ and zero temperature $\beta \rightarrow \infty$.¹ By virtue of the LSZ-reduction formula, one can then translate time-ordered correlation functions of the interacting vacuum to the connected part of the S -matrix elements. The S -matrix is given by Dyson's formula in the interaction picture. It corresponds to the time evolution operator from $t_i = -\infty$, the "in-state", to $t_f = +\infty$, the "out-state". This is the so-called *asymptotic state* formalism. Ingoing states in the asymptotic past t_i are described by free wave packets, they are non-interacting, well-separated single-particle states. The interaction is localized, the particles therefore are free in the asymptotic past. Upon interaction, they scatter into final state particles which are again well separated

¹The former limit is one we will employ in a derivation of kinetic theory from the 2PI formalism of NeqQFT in 3.4. For the comparison of vQFT and NeqQFT objects in the subsequent 3.5, identifying the limits in both frameworks helps us to isolate similar expressions, for example the background field with the VEV in (3.111).

single-particle states with no subsequent interactions. In the asymptotic past and future, the spectrum of the theory exhibits delta-peak structure for the single-particle states with on-shell energies $\omega_p^2 = \vec{p}^2 + m^2$, where, due to self-interactions being present, they have the mass of the full interacting theory.

Already in the first instance of outlining a vQFT, one must specify what is meant by the unperturbed vacuum state corresponding to the lowest energy state of the Fock space for the free theory. In classical statistical field theory, the classical vacuum is the state where literally nothing exists, therefore no fluctuations can take place. On the other hand in quantum field theory, the state defined as the vacuum fluctuates throughout its time evolution. This difference in dynamics has to be considered. Essentially, classical statistical field theory can be obtained from NeqQFT in the limit of large occupations, where structurally the two frameworks have corresponding path integrals which differ by the forms of interaction involved. This difference underlies the mapping from quantum to classical theory, where the initial state of the quantum theory has to conform with the properties of the fluctuating quantum vacuum whilst that of classical theory the properties of the classical vacuum [4]. Conversely, going from classical to quantum theory entails that the dynamics are dominated by the quantum vacuum and the corresponding quantum effective potential, where the classical potential can be neglected as will be important for the distinction of classical spontaneous symmetry breaking (SSB) to SSB in NeqQFT. Considering the dynamical process of SSB in NeqQFT will later on provide us with insight into the dynamics of the background field in a scattering process.

Summarizing, the vQFT asymptotic state formalism essentially constitutes a boundary value problem. This formalism does however not keep track of the dynamics during a scattering event, since it is only concerned with initial and final state products. During a scattering event, as we will elaborate on in 3.2.1, the free particle picture is not applicable anymore and the dynamics of the spectrum of the theory has to be taken into consideration. This is the realm of NeqQFT, which is able to address the real-time dynamics of a system at hand by tracking the evolution of observables from initial conditions to thermalization and beyond.

1.2.2 Nonequilibrium QFT

In contrast to vQFT, the vacuum S -matrix does not exist at finite temperature, because particles do not have an infinite free path length after a collision has taken place. They will interact with something such that assuming the vacuum state in the asymptotic past and future is not valid anymore. The translation between interacting and free vacuum through the adiabatic limit is not possible anymore, as we are explicitly considering a finite temperature.

NeqQFT does not necessitate this subtle translation procedure. As will be elaborated on more thoroughly in 3.2, in NeqQFT correlation functions are described via quantum evolution equations evolved from an initial state $\rho(t_0)$, the initial information is completely contained in this density matrix. Therefore, in comparison to vQFT, NeqQFT

constitutes an initial value problem.

The conventional asymptotic state construction relies on the knowledge of the initial and final state of the system, namely the ground or equilibrium state. This is not possible for general nonequilibrium systems, since the final state is unknown, it is exactly what we are interested in by tracking the time evolution of the system. Since expectation values of observables are necessarily linked to ensemble averages, one can not simply neglect the final state. The Schwinger-Keldysh formalism circumvents the obstruction posed by our lack of knowledge of the final state by introducing a closed-time contour, the *Keldysh* contour \mathcal{C} . The quantum system evolves from a specified initial state forward in time and, subsequently, backwards in the opposite time direction, thereby ending up in the initial state. As a result, the time evolution operator of the system corresponds to a unity operator, but the complexity of the theory increases by requiring one to specify components of correlators on the forward and backward branch of the time evolution respectively. The resulting descriptive theory only requires one to specify the initial density matrix to encompass the complete dynamical information of the system under consideration [5].

In structure, the perturbative expansion of NeqQFT is then identical to that of vQFT, where the time integration is however carried out on the Keldysh contour such that each contour-time-ordered n -point function consists of 2^n components for the two time branches respectively. Further, for NeqQFT initial correlations are present which vanish for the vacuum state. In principle, all orders of correlations can be taken into account, but often it is sufficient to limit oneself to the second cumulant as discussed in 3.2.2 [6]. Since the density matrix can have an arbitrary description, in general translation invariance is lost and a suitable generalized description is obtained by integration along the closed-time Keldysh contour. The reduction of complexity towards vQFT can be achieved by choosing a thermal density matrix $\rho(t_0) \propto e^{-\beta H}$, such that translation invariance is restored $[\rho, P^\mu] = 0$. This choice represents thermal equilibrium. The distribution of particles is then described by Bose-Einstein or Fermi-Dirac statistics, which is contained in the emergence of fluctuation-dissipation relations in thermal equilibrium. Further considering the zero-temperature limit, $\beta \rightarrow \infty$, reduces the equilibrium density matrix to a pure initial state consisting of the interacting vacuum $\rho(t_0) \propto |\Omega\rangle \langle \Omega|$.

Now that we have arrived at thermal zero-temperature QFT, we proceed by constructing asymptotic in- and out states. This asymptotic formalism with $t_i = -\infty$ and $t_f = +\infty$ requires one to only use objects on the forward part of the Keldysh contour. One identifies the forward-forward component of the two-point propagator as the Feynman propagator known from vQFT, i.e. $G^{++} = D_F$ [6]. Vacuum expectation values of correlators are then obtained by

$$\text{Tr} \rho_0 \mathcal{O}^{(H)}(x) \xrightarrow{\beta \rightarrow \infty} \langle \Omega | \mathcal{O}(x) | \Omega \rangle = \langle 0 | \mathcal{T}_{\mathcal{C}} \mathcal{O}^{(I)}(x) S_{\mathcal{C}} | 0 \rangle \quad (1.1)$$

where

$$S_{\mathcal{C}} := \mathcal{T}_{\mathcal{C}} \exp \left[-i \int_{\mathcal{C}} d\tau H_{\text{int}}^{(I)}(\tau) \right] \quad (1.2)$$

is the S -matrix on the Keldysh contour [7]. This step involves identifying the free vacuum via the time evolution operator on the Keldysh contour

$$|\Omega\rangle = U(t_0, -\infty) |0\rangle. \quad (1.3)$$

vQFT makes the so-called *assumption of adiabatic interaction* to go from S_C to S , i.e. to drop the dependence on the Keldysh contour completely. It entails making the ansatz

$$U(-\infty, \infty) |0\rangle = e^{i\nu} |0\rangle, \quad (1.4)$$

such that the free vacuum merely acquires a phase after the entire time-evolution. This assumption essentially constitutes a process of adiabatically switching interactions on sufficiently prior to the observation time and off sufficiently after the observation time such that the system becomes non-interacting again. This leads to the emergence of the conventional S -matrix

$$\langle\Omega| \mathcal{O}^{(I)}(x) |\Omega\rangle = \langle 0| \mathcal{T} \mathcal{O}^{(I)}(x) S |0\rangle e^{-i\nu}, \quad S = \mathcal{T} \exp \left[-i \int_{-\infty}^{\infty} d\tau H_{\text{int}}^{(I)} \right]. \quad (1.5)$$

The usual S -matrix therefore lies solely on the forward-forward branch of the Keldysh contour, as does the Feynman propagator. One can eliminate the phase by introducing suitable in- and out-states as is done in the asymptotic state formalism.

$$|\Omega; \text{out}\rangle = U(t_0, \infty) |0\rangle, \quad \langle\Omega; \text{in}| = \langle 0| U(-\infty, t_0). \quad (1.6)$$

With these definitions, the phase simply drops out in the computation of correlators

$$\langle\mathcal{O}\rangle = \langle\Omega| \mathcal{O}(x) |\Omega\rangle = \frac{\langle\Omega; \text{in}| \mathcal{O}(x) |\Omega; \text{out}\rangle}{\langle\Omega; \text{in}|\Omega; \text{out}\rangle} = \frac{\langle 0| U(\infty, t_0) \mathcal{O}(x) U(t_0, -\infty) |0\rangle}{\langle 0| U(-\infty, \infty) |0\rangle} \quad (1.7)$$

as the denominator reads

$$\langle\Omega; \text{in}|\Omega; \text{out}\rangle = \langle 0| U(-\infty, \infty) |0\rangle = e^{i\nu}. \quad (1.8)$$

Since the operator is inserted after evolution from the infinite past to the time of observation t_0 , only the forward time evolution has to be considered. Physically, the denominator cancels the vacuum loop contributions or disconnected diagrams where the phase ν corresponds to the sum of all vacuum bubbles. Note that this reduction is only possible towards equilibrium and, subsequently, vacuum theory, since the Hamiltonian can acquire a non-adiabatic time dependence driving the system away from equilibrium for general nonequilibrium situations [5].

Interestingly, the theorem that classical field theory corresponds to the sum of all tree diagrams whereas quantum theory incorporates loop corrections, thereby the latter containing the former as depicted in figure 1.1, does not necessarily hold for general nonequilibrium situations. It was conceived for vQFT, where in-medium effects are neglected [4]. Again, we observe that vQFT is contained in the highly complex description of NeqQFT as a limiting case.

1.3 Overview

To separate the application towards Higgspllosion from the developed nonequilibrium strong-field kinetic system, we divided the contents of this thesis into a chapter containing the conventional vQFT description of Higgspllosion [2](#) and one concerned with the derivation of a strong-field kinetic theory from the first principles of nonequilibrium theory and a discussion of particle production mechanisms described therein [3](#).

Having already made a distinction between vQFT and NeqQFT in [1.2](#), [2](#) opens with an introduction for the Higgspllosion phenomenon in vQFT in [2.1](#) and its characteristic features are summarized in [2.2](#). In particular, we will comment on the conventional logic of spontaneous symmetry breaking in [2.3](#), define scattering expressions for a scalar broken ϕ^4 model in [2.4](#) for comparison purposes later on, and subsequently discuss the regime of Higgspllosion in [2.5](#). If the reader is only interested in strong-field kinetic dynamics in the nonequilibrium framework, we recommend to skip this chapter entirely.

[3](#) is instigated with a discussion of the term *particle* in [3.1](#) and a subsequent introduction into NeqQFT for scalar fields in section [3.2](#). For comparison purposes and to provide us with an intuitive and dynamical understanding of spontaneous symmetry breaking in NeqQFT, we summarize its main ideas in [3.3](#). Subsequently, the 2PI equations of motion of NeqQFT will be approximated under the kinetic limit to yield a closed kinetic system for the strong-field regime in section [3.4](#), which will provide the foundation for analysis to understand particle production in this framework.

With this self-consistent set of strong-field kinetic dynamics at our disposal, we venture to isolate mechanisms for particle production in the following section [3.5](#). In this framework, particle production can be facilitated by a collisionless $\mathcal{O}(\lambda^0)$ drift term [3.5.1](#) or by collisional $\mathcal{O}(\lambda)$ inelastic scattering processes as discussed in [3.5.3](#), where the latter is sub-leading in a strong-field coupling counting to the former. Whilst both mechanism facilitate particle production through fluctuations of the strong background field, the latter does so in the language of scattering amplitudes allowing one to discuss generalizations of and make contact with vacuum theory. In the course of analysing the latter, we will gain insight into the connection between vQFT and NeqQFT by defining a translation procedure between the frameworks, in particular in [3.5.2](#) and [3.5.3](#).

Concluding, our results are summarized and prospective research is discussed in [3.6](#).

2 Higgspllosion from the perspective of vacuum QFT

This chapter is supposed to serve the purpose of introducing the conventional Higgspllosion mechanism and the surrounding language. If the reader is solely interested in the derivation of a nonequilibrium strong-field kinetic theory for scalar systems and application thereof to particle production, we recommend to skip this chapter entirely and continue from 3.

Throughout this work, Lorentz indices are Greek letters, contraction of Lorentz vectors is indicated by $(p \cdot s) = \eta_{\mu\nu} p^\mu s^\nu$ with metric signature $(+, -, -, -)$ and we use natural units $\hbar = c = 1$, unless specified otherwise.

2.1 Introduction to Higgspllosion

The standard model of particle physics is one of the most well-established effective theories in physics. Beyond the electroweak (EW) sector, the question arises whether the SM is valid beyond energy domains of 1 TeV. From results of lattice computations, we know that the bare Lagrangian must consist of parameters which have to be tuned very precisely to accurately produce the particles of the SM whose masses are much less than 1 TeV [8]. Such a fine-tuning is considered to be technically unnatural, challenging the validity of the SM for the ultraviolet (UV) regime.

Predictions for beyond the standard model (BSM) phenomena possibly completing the UV sector of the SM have so far not been met by extensive searches at the LHC. Apart from the Planck scale, currently there does not exist a fundamental energy scale at which new BSM physics might appear. Being the only scalar degree of freedom in the SM, the Higgs boson might pose a means to providing answers to this question [9–11].

Possible further obstructions to the validity of the SM are posed by unitarity violations in multi-particle amplitude computations. This is a feature exhibited by a wide class of weakly coupled theories, the simplest example being $\lambda\phi^4$ -theory. Considering the decay process of one highly energetic (virtual, indicated by a star superscript) particle into very many final states of the same particle, the number of final state particles being the *multiplicity*,

$$\varphi^* \rightarrow \varphi^n,$$

a high multiplicity is suppressed by a high power of the coupling constant, which is small $\lambda < 1$. Since graphs do not destructively interfere in this scalar theory, the number of graphs does at the same time grow factorially. The resulting square amplitude will therefore be proportional to $n!\lambda^n$, where the resulting observables will become large

for $n > 1/\lambda$. This argument has motivated perturbative and semi-classical ventures to test higher order amplitudes [12]. In the particular case for the double-scaling limit $n \rightarrow \infty$, $\lambda \rightarrow 0$ with $n\lambda$ held fixed in the vicinity of the kinematical threshold, where all final particles are at rest, the corresponding rate¹ has been shown to scale exponentially $\mathcal{R} \sim \exp[F(n\lambda)/\lambda]$ [13]. The sign of the function F depends on the dynamical regime of energies, or correspondingly multiplicities, of the process. The implied violation of unitarity at large n poses a question to the validity of these efforts, where the extrapolation of low n expressions to high n is ill-posed, neglecting possible suppressions by processes arising at higher order.

One possible alleviation to the problem of observable large cross sections for the production of a high number of weakly-interacting bosons in the multi-TeV regime has been proposed by a *Higgspllosion* and related *Higgsperision* mechanism [1]. It proposes the final state of the decay of a very heavy electroweak object to be dominated by the production of very many Higgs, W and Z bosons. This enhancement of a decay channel with very high multiplicities leads to a strong suppression of the resummed propagator by virtue of the optical theorem. The associated energy scale, called the *Higgspllosion* scale, emerges where the corresponding squared amplitudes become exponentially large [14]. This suppression poses as an effective cut-off for loop processes above the *Higgspllosion* scale, such that this mechanism leads to an asymptotically safe theory [15] and could even address the Higgs hierarchy problem. Therefore, the exponential growth of amplitudes calculated perturbatively and semi-classically is mitigated by a simultaneous suppression of the resummed propagator, preventing the growth to ever violate perturbative unitarity.

2.2 Characteristic features of Higgspllosion

In the set-up of *Higgspllosion* [1, 14–16], we are considering a highly virtual initial state φ^* with $p^2 \gtrsim (nm)^2 \gg m^2$ decaying into n non-relativistic final states φ^n . A large momentum transfer takes place from the initial to the final state. *Higgspllosion* does not describe a tree-level process, the initial state is highly virtual and therefore off-shell with respect to the renormalized vacuum mass. We can then identify *Higgspllosion* as an intermediate process at loop order, where one highly off-shell propagating degree of freedom decays very quickly in a multi-particle state, consisting of n on-shell soft particles. We stress this again, that the initial state is not an on-shell one-particle state, it is a composite state with a broad width, therefore decaying rapidly into the final state. The regime of *Higgspllosion* is one of high multiplicities n

$$n \gg \frac{1}{\lambda} \gg 1.$$

¹The rate \mathcal{R} corresponds to an integration of the squared amplitude over the Lorentz invariant phase space of the process. Subject to suitable normalization, the rate is then proportional to the corresponding decay rate and cross section.

Including one-loop effects, the rate of this process was found to exponentiate in the double-scaling limit² as

$$\mathcal{R} = \exp \left\{ \frac{\lambda n}{n} \left[\log \frac{\lambda n}{4} + 3.02 \sqrt{\frac{\lambda n}{4\pi}} - 1 + \frac{3}{2} \left(\log \frac{\epsilon}{3\pi} + 1 \right) - \frac{25}{12} \epsilon \right] \right\}. \quad (2.1)$$

The rate, and therefore related observables, grow exponentially above the characteristic Higgsplosion scale $E_* = \mathcal{O}(25 - 100)$ TeV

$$\mathcal{R} \begin{cases} \ll 1 & p^2 \lesssim E_*^2 \\ \gg 1 & p^2 > E_*^2. \end{cases} \quad (2.2)$$

We comment here that such an exponential behaviour is well known in nonequilibrium theory from the decay of a scalar strong-field into particles, which will be elaborated on in the later analysis 3.5.1. The decay width of the above process is now proportional to the rate (2.1) and will thus diverge for momenta above the characteristic Higgsplosion scale

$$\Gamma \propto \mathcal{R} \rightarrow \infty \quad \text{as} \quad p \rightarrow \infty.$$

With the initial composite state being far away from the energy shell $p^2 \gg m^2$, this propagating degree of freedom requires a finite width to appear in the propagator, corresponding to the deviation of the on-shell delta peak in the underlying spectral function³. Discussing the particle picture around an intermediate state is subtle in a real-time formalism, since we do not observe these. We will comment further on the particle interpretation in 2.1.

Through the optical theorem, the divergence of the decay width will translate to a divergence of the imaginary part of the self-energy $\text{Im} \Sigma^4$.

The decay width however also enters the renormalized Dyson propagator via the optical theorem such that the propagator is effectively suppressed for momenta above the Higgsplosion scale

$$\Delta_R(p) = \frac{i}{p^2 - m^2 + im\Gamma(p^2)} \rightarrow 0 \quad \text{as} \quad p \rightarrow \infty. \quad (2.3)$$

The Higgsplosion mechanism, namely the strong growth of the rate with multiplicities, is then well-controlled, as physical observables will be tamed by the corresponding Higgsplosion mechanism, which describes the effective suppression of propagating degrees of freedom through the divergence of the rate, and therefore decay width, in the propagator. This was exemplified for cross-sections in a gluon-fusion process, which

² $n \rightarrow \infty$ and $\lambda \rightarrow 0$ with $n\lambda$ held fixed.

³The to-be-employed kinetic theory will not be able to treat this regime, since kinetic theory requires an on-shell particle picture facilitated by a delta-shaped width in the spectral function. Therefore, the focus of our work is rather to make a first connection to the language of scattering amplitudes in nonequilibrium through a strong-field kinetic theory than to identify and analyze Higgsplosion in a nonequilibrium setting. The latter objective will have to be the subject for future work.

⁴This poses the question of validity for the underlying physical system to define a localizable QFT [17], which was contested in [18]

would set-up the Higgspllosion scenario as

$$gg \rightarrow h^* \rightarrow h^n,$$

where the cross-section reaches an observable level below and will be suppressed for energies above the Higgspllosion scale

$$\sigma_{gg \rightarrow h^n} \propto \begin{cases} \mathcal{R} & \mathcal{R} < 1 \text{ Higgspllosion} \\ \mathcal{R}^{-1} & \mathcal{R} \gg 1 \text{ Higgspllosion} \end{cases} \rightarrow 0 \quad \text{as } p^2 \rightarrow \infty. \quad (2.4)$$

The suppression of the propagator above the Higgspllosion energy scale leads to asymptotically safe couplings in the UV and a cut-off for UV loop integrals [1].

Let us comment here that the surrounding discussion of perturbative unitarity is not applicable for a nonequilibrium analysis. As we will see later on, in the strong-field regime of nonequilibrium theory one can only define dynamical and local scattering amplitudes. To be specific, one can isolate an object which has the interpretation of a squared scattering amplitude for certain regimes, this object does not necessarily suffice this interpretation globally. This is not a drawback of nonequilibrium theory, it is more general and therefore encompasses notions of vacuum theory in certain limits. Requiring unitarity to hold is therefore only valid for certain regimes, because $|\mathcal{M}|^2$ can not always be defined. One thus to make the subtle distinction between whether unitarity is violated or whether we are in a regime where one can not define an object which locally has the conventional interpretation of a scattering amplitude. Testing perturbative unitarity to hold in nonequilibrium is therefore not a solid requirement for validity since its total probabilistic interpretations is not necessarily globally defined in the first place.

2.3 Spontaneous symmetry breaking and Goldstone's theorem

In this section we want to outline the conventional logic of spontaneous symmetry breaking in vQFT.

If a field takes on a non-zero global value, it could violate a symmetry of the Lagrangian leading to it being *spontaneously broken*. Spontaneous symmetry breaking (SSB) occurs for a theory with degenerate ground state, where a particular choice of vacuum does not respect the underlying symmetry of the theory. This subject is treated in any conventional QFT textbook, for example [2].

Consider real scalar quartic theory for N fields which is symmetric under the continuous, global $O(N)$ symmetry

$$\mathcal{L} = \frac{1}{2} \partial^\mu h \circ \partial_\mu h - V(h), \quad V(\phi) = \frac{1}{8} g(h^2 - v^2) > 0, \quad (2.5)$$

where $h^2 \equiv h \circ h \equiv \sum_r h_r h_r$. For a non-vanishing ground state $h_r = v$, the minimum of this potential does not coincide with the origin but rather anywhere on the vacuum manifold S^{N-1} defined by $h^2 \stackrel{!}{=} v^2$. The extremum of the potential at $h = 0$ is meta-stable, where quantum fluctuation lead the system to decay into one of the stable vacuum

configuration on \mathbb{S}^{N-1} . This choice of vacuum breaks the symmetry $O(N) \rightarrow O(N-1)$, where the residual symmetry corresponds to the remaining $(N-1)$ flat directions $h_0 = (0, \dots, 0, v)$. Employing a mean-field approach $h(x) = v + \varphi(x)$, we can write this as

$$h = (h_\perp, v + \varphi), \quad h_\perp = (h_1, \dots, h_{N-1}). \quad (2.6)$$

The *Goldstone theorem* now says that for a QFT with a global continuous symmetry group G , the SSB to the stability group H implies the existence of $(\dim G - \dim H)$ massless scalars, the *Goldstone bosons*. For our theory, we obtain one massive field f and $(N-1)$ massless fields h_\perp , where the latter are the Goldstone modes. Note that this distribution of mass to different modes is contained in the mass matrix

$$\mathcal{M}_{sr} = \frac{\delta^2}{\delta h_r \delta h_s} V(h)|_{h=h_0}. \quad (2.7)$$

From another perspective, the one direction longitudinal to the sphere is non-vanishing such that the potential $V(h)$ has non-zero curvature, this implies a non-vanishing mass matrix giving rise to a massive scalar.

2.4 Broken scalar ϕ^4 theory

It will be instructive and useful for later comparison reasons to review a scalar model with SSB, where we will consider a single real scalar field $h(x)$ with VEV $\langle h \rangle = v$

$$\mathcal{L} = \frac{1}{2} \partial^\mu h \partial_\mu h - \frac{\lambda}{4} (h^2 - v^2)^2. \quad (2.8)$$

We make a mean field ansatz $h(x) = \varphi(x) + v$, with $\langle \varphi \rangle = 0$, such that

$$\mathcal{L} = \frac{1}{2} \partial_\mu \varphi \partial^\mu \varphi - \frac{m^2}{2} \varphi^2 - \lambda v \varphi^3 - \frac{\lambda}{4} \varphi^4, \quad (2.9)$$

with $m = \sqrt{2\lambda}v$. The equation of motion reads

$$-[\Box_x + m^2]\varphi = 3\lambda v \varphi^2 + \lambda \varphi^3. \quad (2.10)$$

Note that parametrically we have $v \sim 1/\sqrt{\lambda}$ since the field scales like $\varphi \sim 1/\sqrt{\lambda}$, which can be concluded from the minimum of the potential

$$0 \stackrel{!}{=} V(\varphi) \Leftrightarrow 0 = \varphi \left[\lambda \varphi^2 + 3\lambda v \varphi + m^2 \right] \Leftrightarrow \varphi_\pm \propto \frac{1}{\sqrt{\lambda}}.$$

This theory (2.9) exhibits two kinds of self-interactions, an effective cubic vertex and the conventional quartic vertex

$$\begin{array}{c} \diagup \\ \bullet \\ \diagdown \end{array} = -i\lambda v, \quad \begin{array}{c} \diagup \\ \times \\ \diagdown \end{array} = -i\lambda. \quad (2.11)$$

2.4.1 Decay rate

The Higgspllosion phenomenon describes the behaviour of observables in the decay process of a highly virtual mode $1^* \rightarrow n$, where the mode of decay is dominated by the cubic vertex.

As noted above, the field parametrically scales as $\phi \sim 1/\sqrt{\lambda}$, one therefore has to be careful when counting the order of the coupling for a given contribution. For example, one counts $\mathcal{O}(\lambda v) \sim \mathcal{O}(\lambda/\sqrt{\lambda}) = \mathcal{O}(\sqrt{\lambda})$.

At tree level $\mathcal{O}(\lambda)$, the decay process of an initial particle state to two final particle states

$$\begin{array}{c} k_2 \\ \diagup \\ p \text{---} \bullet \\ \diagdown \\ k_3 \end{array} \rightarrow \langle \vec{k}_2 \vec{k}_3 | iT | \vec{p} \rangle = (2\pi)^4 \delta(p - k_2 - k_3) i\mathcal{M}(p, k_2, k_3)$$

has the following associated decay width

$$\begin{aligned} \Gamma_{p \rightarrow k_2 + k_3}^{\text{vac}}(\vec{p}) &= \frac{1}{2!} \frac{1}{2\omega_{\vec{p}}} \int \frac{d^3 k_2}{(2\pi)^3 2\omega_{\vec{k}_2}} \frac{d^3 k_3}{(2\pi)^3 2\omega_{\vec{k}_3}} (2\pi)^4 \delta^{(4)}(p - k_2 - k_3) |\mathcal{M}(p, k_2, k_3)|^2 \\ &= \frac{1}{2} \frac{1}{2\omega_{\vec{p}}} \int \frac{d^3 k_2}{(2\pi)^3 2\omega_{\vec{k}_2}} \frac{d^3 k_3}{(2\pi)^3 2\omega_{\vec{k}_3}} (2\pi)^4 \delta^{(4)}(p - k_2 - k_3) \lambda^2 v^2, \end{aligned} \quad (2.12)$$

where the factor $1/2!$ stems from the identical final state particles. The initial state p is here on-shell with respect to the physical, renormalized vacuum mass, $p^2 = m_{\text{R,vac}}^2$ such that this decay process is kinematically forbidden at tree-level. This is not the case for a dynamically participating background field with unconstrained energy variable, which is accounted for automatically nonequilibrium theory. Later on in 3.5.3, we will explicitly demonstrate how this process arises upon including the background field as a dynamical energy reservoir. This process does not describe Higgspllosion, but will serve the purpose of identifying expressions for decay rates in nonequilibrium theory later on in 3.5.3. Through this endeavour, we will find an explicit mechanism by which one can reduce scattering expressions including a dynamical background field from nonequilibrium to vacuum theory.

2.5 The regime of Higgspllosion

In this section we want to motivate why we are explicitly considering strong-field kinetic dynamics for analysing Higgspllosion.

Due to its initial conditions, Higgspllosion is expected to be a near-equilibrium phenomenon. Whether it is intrinsically perturbative in the coupling or also arises within the non-perturbative regime is not clear as of yet [18]. Addressing this question is however not the purpose of the present work. This thesis solely aims to make contact with Higgspllosion for future investigations by discussing strong-field particle production phenomena in a strong-field scalar kinetic framework.

What we will observe in the course of this thesis is that a high number of final state particles only emerges to very high loop order, a $\mathcal{O}(\lambda)$ coupling analysis only encompasses $1 \rightarrow 2$ processes as found in section 3.5. Higgspllosion arises by considering scattering rates, which are objects dealing with the linear response of a single mode in the spectrum, it can therefore inherently not be a non-thermal phenomenon [19]. Higgspllosion takes place for a system close to equilibrium, which will allows us to impose approximations.

Further, we have to account for strong-field dynamics, since Higgspllosion is a strong-field phenomenon. Following [1, 14], we expect the Higgspllosion energy scale to be greater than $E_* \geq 100m$, where m is the mass of one final state particle. The original calculation for multi-particle production $\varphi^* \rightarrow \varphi^n$ was at the kinematic threshold and therefore assumed n final state particles at rest such that $n = E_*/m$. This calculation was extended in the vicinity of the kinematic threshold with the n final state particles having a mean non-relativistic energy of $\epsilon \ll 1$ resulting in $E_*/m = n(1 + \epsilon)$. Following [1], the multiplicity for this particle production process is large $n \sim 1/\lambda$, as $\lambda < 1$, which implies that for the Higgspllosion scale we have $E_* \sim 1/\lambda$. If now the non-kinetic term in the action becomes comparable to the kinetic term, one can not perform conventional perturbation theory with propagators. This is the *strong-field* regime for a scalar field φ . With $E_* \sim 1/\lambda$, this implies that parametrically the field has $\varphi \sim 1/\sqrt{\lambda}$ for strong fields. This agrees with the classical ground state values of the VEV being $v \sim 1/\sqrt{\lambda}$, as we haven seen by considering classical φ^4 theory with SSB. With the smallness of the Higgs self-coupling $\lambda < 1$ [11], the strong-field has therefore to be accounted for exactly.

To make the connection with vacuum theory, an explicit particle picture is necessary which is facilitated by kinetic theory. Therefore, in order to study particle production mechanisms including strong-field dynamics, a strong-field kinetic description derived from the first principles of nonequilibrium theory is necessary and will be derived in the following.

3 Particle production in nonequilibrium strong-field kinetic theory

We will now attempt to derive a self-consistent scalar kinetic system for the strong-field regime in 3.4 from the first principles of nonequilibrium QFT introduced in 3.2. This description will encompass collisionless and collisional particle production processes which are explicitly driven by the strong-field. To this end, we discuss the mechanisms of particle production for the strong-field regime facilitated by the derived kinetic system in a subsequent analysis 3.5, where a full account of the particle production dynamics starting from initialization towards thermalization is presented in the conclusion 3.6.

3.1 Concerning particles

Historically, a particle concept has been at the centre of developing quantum field theory. Eluded to by the misnomer "second quantization", the original motivation for a quantization of classical field theory stemmed from the successful efforts of quantizing classical point mechanics in the form of quantum mechanics, where the latter was conceived as a theory of discretized and *localized* energy packets, quanta.

As was already discussed in the introductory comparison 1.2, originally particles were defined as the representations of Fock states built from the free theory. This is inherently linked to the notion of a vacuum. In this framework, particles are built as representations of states which are not the vacuum state, where the latter is defined as the state not containing any particles for all momenta and times. However, this framework relies on free theory and a corresponding mode decomposition of the free field facilitated by a free equation of motion. Introducing interactions, such a mode decomposition is inaccessible due to non-linear sources appearing in the equation of motion. This leads to the realization that the representations of states corresponding to interacting fields are physically distinct from the ones of free fields, demonstrated by the absence of a unitary mapping between the two. Furthermore, a unique vacuum does not in general exist in the presence of interactions, since phase transitions between different vacuum configurations are facilitated by interactions.

Following our initial discussion 1.2, the free theory particle concept is restored in interacting theory by virtue of the asymptotic state formalism, where the unitary S -matrix operator provides a mapping between the asymptotic past to the asymptotic future, respectively prior and after interactions could occur. This is technically realized by the discussed adiabatic switching of interactions.

If one solely resorts to phenomenological collider calculations, such a particle picture

centred on a perturbative treatment around free theory suffices. Otherwise, this particle picture constructed by requiring locality and an inherent invariance under symmetry operations yielding characteristic conserved charges has to be challenged.

A different concept exists in in medium, that of *quasi-particles*. This is a collective noun describing all excitations emerging from local interactions of the microscopic degrees of freedom (for example, phonons and plasmons). Apart from localization, particles and quasi-particles describe the same phenomenon, where the latter however crucially describes an *emergent* phenomenon. Such an understanding raises conceptual questions, namely how the conventional criterium of locality is to be understood.

These questions are testing the chain of reasoning under which the conventional particle picture is conceived. The demand for reconciliation is therefore at the fundamental level of constructing a suitable QFT able to address these problems.

Possible alleviation is presented in the form of the to-be-employed Schwinger-Keldysh formalism of nonequilibrium QFT. Conceptually, this framework encompasses the environment into the closed system description by including energy transfer with the environment into the dynamics, there is no conceptual difference between the environment and the system. Such a description allows for noise to be self-consistently produced by the quantum fluctuations of the system, thereby serving as a catalyst for dynamics and for feedback effects between the quantum system and its environment. From another point of view, this description challenges vacuum concepts, because any form of medium has to be external in vacuum theory. This formalism concentrates on the underlying statistical approach of statistical field theory, namely that of correlation functions and fluctuations in a general sense. Having access to the real-time dynamics of the resummed one- and two-point function allows us to take a high degree (in principle exact) of these correlations into account [20].

Crucially, the particle picture is now defined effectively from field fluctuations defined by the dynamical evolution of the correlators defining the theory. If one were able to solve the exact dynamics of such a system, the concept of a particle would be superfluous. Such an approach therefore renders the particle an emergent phenomenon for a weakly interacting system close to vacuum (dilute).

In particular, this dynamical particle concept is facilitated by the spectral function ρ , which encodes the spectrum of the theory and is a dynamical object self-consistently coupled to the system. This object exists in vQFT in a non-dynamical form, where a particle picture is facilitated by delta-peaks in the spectrum. Each peak corresponds to a particle species, its width to the corresponding lifetime, and the peak position to the mass for $|\vec{p}| = 0$ and to the dispersion relation for non-vanishing momenta. For a finite width, the particle peak can be described by the Breit-Wigner formula. However, as we will see in the following 3.2.5, the nonequilibrium frameworks allows one to consider finite, general widths beyond Breit-Wigner form and, crucially, *dynamical* modifications of these peaks, where the conventional particle picture of vQFT is tested. The particle picture is facilitated around distinct peaks in the spectral function which can however dynamically change due to interactions causing the position and the width to be modified, thereby reducing the intuitive picture of particles colliding to a flow of energy fluctuations in the system on infinitesimal scales. Only where a sufficient separation

between interaction time scales and mean free path of propagating degrees of freedom applies can these complex dynamics approximately be treated with an emergent particle picture, facilitated by an effective description such as kinetic theory for weakly interacting system which are dilute.

3.2 Nonequilibrium quantum field theory for scalar fields

This section serves the purpose of introducing and illustrating the core ideas of the 2PI formulation of the real-time Schwinger-Keldysh NeqQFT formalism. The following presentation for the remainder of this section is a summarized version of the presentation given in [21, 22], if not specified otherwise.

3.2.1 Generalizing the vacuum framework

As has been eluded to in 1.2, NeqQFT is concerned with the real-time dynamics of observables for a given initial state parametrized by a density matrix $\hat{\rho}$ with distributional properties

$$\rho^\dagger = \rho, \quad \text{Tr} \rho = 1, \quad \langle \rho \rangle \leq 1. \quad (3.1)$$

The evolution of the density matrix is described by the von Neumann equation, whose solution is contained in the unitary time evolution operator $\hat{U}(t, t')$, such that $\hat{\rho}(t) = \hat{U}(t, t_0) \hat{\rho}_0 \hat{U}(t_0, t)$. We are interested in physical observables which are given by the expectation value of a corresponding operator \hat{O} at time t by

$$\langle \mathcal{O}(x) \rangle = \frac{\text{Tr} \left\{ \hat{O}(x) \hat{\rho}(t) \right\}}{\text{Tr} \hat{\rho}(t)} = \frac{\text{Tr} \left\{ \hat{O}(x) \hat{U}(t, t_0) \hat{\rho}_0 \hat{U}(t_0, t) \right\}}{\text{Tr} \hat{\rho}_0}. \quad (3.2)$$

As was explained in 1.2, we now introduce the closed-time Keldysh contour \mathcal{C} to bypass the specification of a final state. Technically, this is achieved by inserting a unity operator in the above equation, $\hat{1} = \hat{U}(t, \infty) \hat{U}(\infty, t)$, which leads to an evolution that starts at the initial time t_0 , runs forwards along the real-time axis and then returns back to t_0

$$\langle \hat{O}(t) \rangle = \frac{\text{Tr} \left\{ U(t_0, \infty) U(\infty, t) \hat{O} \hat{U}(t, t_0) \hat{\rho}_0 \right\}}{\text{Tr} \hat{\rho}_0}. \quad (3.3)$$

This expectation value will be specified as usual by the introduction of a generating functional, which requires us to provide suitable initial conditions.

3.2.2 The initial conditions

The following treatment of initial conditions is taken from [23] if not specified otherwise.

Fixing particular initial conditions allows us to specify a corresponding experimental set-up and is therefore at the core of analysing the dynamical evolution of the system

at hand. A general initial density matrix can be arbitrarily complex, where certain special cases provide an immense reduction of complexity. This reduction is facilitated by the dephasing of off-shell elements of the initial density matrix, resulting in an effective diagonalization in a suitable basis for sufficiently late-times [24]. For example, thermal theory diagonalizes the density matrix in the energy eigenbasis by assuming the form $\rho_D \propto e^{-\beta H}$, whereas vQFT assumes a pure vacuum initial state $\rho_D \propto |\Omega\rangle \langle \Omega|$ which is synergetic with the asymptotic state construction. Making a suitable choice for the initial density matrix decides over the degrees of freedom accessible for dynamical evolution. A general nonequilibrium initial state does not exhibit the symmetries commonly assumed in vQFT. If the initial state is invariant under symmetries, there exist constraints on the form of density matrix to be employed. In particular, a thermal density matrix restores time translation invariance by satisfying

$$[e^{-\beta H}, P^\mu] = 0 \quad (3.4)$$

for the generator P^μ of translations $\mathcal{O}(x+a) = e^{ia \cdot P} \mathcal{O}(x) e^{-ia \cdot P}$, and the Hamiltonian $H = P^0$. A general nonequilibrium density matrix does not suffice this commutator

$$[\rho_0, P^\mu] \neq 0. \quad (3.5)$$

The reduction of complexity necessary to go from general NeqQFT to vQFT can be illustrated by virtue of a reduction of complexity in the density matrix

$$\rho_0 \xrightarrow{\text{thermalization}} \frac{e^{-\beta H}}{\text{Tr} e^{-\beta H}} \xrightarrow{\beta \rightarrow \infty} |\Omega\rangle \langle \Omega|. \quad (3.6)$$

For the to-be-introduced 2PI formalism of NeqQFT, we shall employ Gaussian initial conditions, which only depend on one- and two-point functions and initial conditions thereof. They encompass all free particle states of the asymptotic description. Since they encompass a broad class of mostly statistically uncorrelated initial conditions, a Gaussian density matrix will suffice for a description of the Higgspllosion phenomenon. Furthermore, wide classes of initial conditions lead to the same effective descriptions by a virtue of loss of sensitivity on the initial conditions. This reduction of complexity takes place in the course of *thermalization*, which describes the evolution towards thermal equilibrium. Understanding thermalization lies at the core of understanding this loss of sensitivity on the underlying microscopic degrees of freedom leading towards effective descriptions, which are at the core of pushing the frontier of yet unanswered fundamental questions.

3.2.3 Correlation functions

Physical observables are constructed from fields and correlation functions in QFT by virtue of a generating functional

$$\begin{aligned}
 Z[J, R, \rho_0] &= e^{iW[J, R, \rho_0]} \\
 &= \underbrace{\int \mathcal{D}\varphi_0^- \mathcal{D}\varphi_0^+ \langle \varphi^+ | \rho_0 | \varphi^- \rangle}_{\text{initial conditions}} \underbrace{\int_{\varphi_0^+}^{\varphi_0^-} \mathcal{D}\varphi e^{i[S[\varphi] + \int_{x,C} J(x)\varphi(x) + \frac{1}{2} \int_{xy,C} \varphi(x)R(x,y)\varphi(y)]}}_{\text{quantum dynamics}},
 \end{aligned} \tag{3.7}$$

where we use the notation $\int_{x,C} = \int_C dt \int d^3x$. This presentation of the generating functional and the equations of the one- and two-point function are explicitly taken from [22]. J and R are linear and bilinear external source terms, respectively. Extending the framework of vQFT, the generating functional (3.7) of nonequilibrium QFT incorporates the quantum fluctuations from the dynamics and, additionally, statistical fluctuations from averaging over the initial conditions ρ_0 . Note that φ_0^\pm are the eigenstates of the field operator at time t_0 for both branches of the Keldysh contour. Furthermore, a bilinear source term appears here as it will provide us with a means to generate the propagator via functional derivatives, which is the object of interest for the later on introduced 2PI formalism commonly employed in nonequilibrium QFT.

Note that choosing Gaussian initial conditions, the Gaussian density matrix can be absorbed in the sources J, R of (3.7) such that

$$Z[J, R] \equiv Z[J, R; \rho_0 = \rho_{0,\text{Gauss}}] = \int \mathcal{D}\varphi e^{iS[\varphi] + i\varphi J + \frac{i}{2} \varphi R \varphi} \tag{3.8}$$

which is then of the familiar vacuum form but with the time integration contour replaced by the Keldysh contour \mathcal{C} , if not specified otherwise. Instead choosing more general initial conditions amounts to the appearance of higher order source-times and, correspondingly, higher order initial correlation functions which have to be taken into account¹.

Within NeqQFT, correlation functions which are time-ordered along the Keldysh contour are now produced from the generating Schwinger functional by taking suitable functional derivatives with respect to source terms and setting the sources to zero afterwards. In particular, the one-point function, which will also be referred to as the *background* (or mean) field, can be expressed as

$$\phi(x) = \langle \hat{\varphi}(x) \rangle = \frac{\delta W[J, R]}{\delta J(x)} \Big|_{J, R=0}. \tag{3.9}$$

Being the expectation value of the field, the background field gives us the nonequilibrium pendant to the VEV v in vQFT. This has to be distinguished from the vacuum *state* of vQFT, which corresponds to the ground state of the free Fock space defined by being the kernel of the annihilation operator $a|\text{vac}\rangle = 0$. In contrast for NeqQFT, exploring

¹It is not clear how suitable Gaussian initial conditions are in general since taking higher-order initial correlation functions into account can lead to a substantial modification of the dynamics [25].

the structure of the dynamical vacuum for strong fields requires taking the dynamics of the background field into account. When saying *vacuum* in nonequilibrium theory, we imply the presence of a background field in the absence of particles. The vacuum is historically associated with the state which is characterised by being unoccupied, exhibiting all internal symmetries of the theory and the lowest energy state. However, the vacuum itself is a dynamical object and its internal structure as well as its time evolution have to be taken into account in any self-consistent description [26].

The connected two-point function, i.e. the selectively *resummed* propagator, can be written as

$$G(x, y) = \langle \mathcal{T}_C \hat{\phi}(x) \hat{\phi}(y) \rangle - \phi(x)\phi(y) = 2 \frac{\delta W[J, R]}{\delta R(x, y)} \Big|_{J, R=0} - \phi(x)\phi(y). \quad (3.10)$$

One can decompose the full propagator (3.10) into its antisymmetric (real) and symmetric (imaginary) part, explicitly

$$G(x, y) = F(x, y) - \frac{i}{2} \rho(x, y) \text{sgn}_C(x^0 - y^0), \quad (3.11)$$

where

$$F(x, y) = \frac{1}{2} \langle \{ \hat{\phi}(x), \hat{\phi}(y) \} \rangle - \phi(x)\phi(y), \quad (3.12)$$

$$\rho(x, y) = i \langle [\hat{\phi}(x), \hat{\phi}(y)] \rangle, \quad (3.13)$$

and $\text{sgn}_C(x^0 - y^0)$ is ± 1 depending on whether x^0 is after or before y^0 along the Keldysh contour [22]. The cost associated to the appearance of the Keldysh contour is that one has to specify the components of any object on the forward \mathcal{C}^+ and backward \mathcal{C}^- branch of the contour. Conveniently, the decomposition (3.11) allows us to circumvent this distinction by virtue of sgn_C , which is why we will employ a similar decomposition for the necessary two-point functions we encounter.

The expectation value of the commutator, $\rho(x, y)$, is the spectral function of the theory and the anti-commutator, $F(x, y)$, denotes the statistical propagator. Both are real functions but differ in symmetry properties

$$F(x, y) = F(y, x), \quad \rho(x, y) = -\rho(y, x). \quad (3.14)$$

Physically, the spectral function encodes information about the spectrum of the theory, it contains information about available states and is subject to the equal-time commutation relations [22]

$$\rho(x, y)|_{x^0=y^0} = \partial_{x^0} \partial_{y^0} \rho(x, y)|_{x^0=y^0} = 0, \quad \partial_{x^0} \rho(x, y)|_{x^0=y^0} = \delta^{(3)}(\vec{x} - \vec{y}), \quad (3.15)$$

which emerge due to quantising the underlying theory in equal time slices. The spectral function is normalized by virtue of these relations. As eluded to in 3.1, the spectral function lies at the core of a particle description. As we will see in the following, the 2PI formalism of NeqQFT provides us with a complete description of the dynamics of

the spectral function encoded in the variational principle (3.16), where an exact solution would encode the complete, inhomogeneous dynamics of a collision event.

The statistical propagator on the other hand provides information about how the states are occupied. As F measures how the states are occupied, it can be employed to parametrically define an explicit time-dependent occupation number as we will do when formulating kinetic theory around (3.32).

3.2.4 The effective action

Following [22], the 2PI effective action $\Gamma[\phi, G]$ is defined as the double Legendre transform of the connected generating functional $W[J, R]$ with respect to the sources,

$$\Gamma[\phi, G] = W - \int_{x, \mathcal{C}} J(x) \frac{\delta W}{\delta J(x)} - \int_{xy, \mathcal{C}} R(x, y) \frac{\delta W}{\delta R(x, y)}.$$

In contrast to the 1PI effective action, here the equations of motion for one- and two-point functions result from the stationary principle

$$\frac{\delta \Gamma}{\delta \phi(x)} = 0, \quad \frac{\delta \Gamma}{\delta G(x, y)} = 0. \quad (3.16)$$

Importantly, the one- and two-point functions already take their physical and resummed values at these stationary points. These coupled integro-differential equations of motion in conjunction with Gaussian initial conditions provided to the one- and two-point function defining the theory, namely ϕ and $G = (F, \rho)$, facilitate the foundation for solving for the dynamics of any observable. They are the core of the initial value problem constituted by NeqQFT.

Having chosen Gaussian initial conditions, the 2PI effective action for a scalar theory with one-point function ϕ and full propagator G can be written as [22]

$$\Gamma[\phi, G] = S_C[\phi] + \frac{i}{2} \text{Tr}_{\mathcal{C}} \ln G^{-1} + \frac{i}{2} \text{Tr}_{\mathcal{C}} \left\{ G_0^{-1}(\phi) G \right\} + \Gamma_2[\phi, G] + \text{const}. \quad (3.17)$$

In contrast to a vQFT framework, the time arguments of the constituents are all elements of the Keldysh contour. G_0^{-1} is the inverse classical propagator, defined by the classical action

$$iG_0^{-1}(x, y; \phi) = \frac{\delta^2 S_C[\phi]}{\delta \phi(x) \delta \phi(y)}. \quad (3.18)$$

$\Gamma_2[\phi, G]$ contains all 2PI diagrams without external legs beyond the one-loop level [27]. 2PI graphs are those that do not become disconnected after removing two inner propagator lines. As we will discuss later on 3.5, the two-loop contributions Γ_2 will facilitate collisional particle production whereas collisionless particle production is driven by one-loop effect of fields through a drift term corresponding to $\frac{\delta \frac{i}{2} \text{Tr} G_0^{-1} G}{\delta G}$.

Following the treatment reviewed in [22], we will derive all objects of interest for the quantum field theory of a real, N -component scalar field φ_a ($a = 1, \dots, N$) with $O(N)$ -

symmetric classical action

$$S[\varphi] = \int_{x,\mathcal{C}} \left[\frac{1}{2} \partial^\mu \varphi_a(x) \partial_\mu \varphi_a(x) - \frac{m^2}{2} \varphi_a(x) \varphi_a(x) - \frac{\lambda}{4!N} (\varphi_a(x) \varphi_a(x))^2 \right] \quad (3.19)$$

Here summation over repeated indices is implied as well as the integration over the Keldysh contour \mathcal{C} . In order to get the similar set-up for Higgspllosion, we will, for the purposes of our analysis, set $N = 1$ and consider the case of a non-vanishing field expectation value. Note that explicitly $N = 4$ already describes the Higgs sector of the SM [28].

Performing a shift $\varphi \rightarrow \phi + \varphi$, the interaction part of the action (3.19) is given by

$$iS_{int}[\varphi; \phi] = - \int_{x,\mathcal{C}} i \frac{\lambda}{6N} \phi_a(x) \varphi_a(x) \phi_b(x) \varphi_b(x) - \int_{x,\mathcal{C}} i \frac{\lambda}{4!N} (\varphi_a(x) \varphi_a(x))^2. \quad (3.20)$$

As can be seen, the presence of the background field generates an effective cubic interaction vertex. Comparing with (2.9), this additionally provides us with a comparable set-up to conventional Higgspllosion in vacuum QFT.

3.2.5 Evolution equations

The 2PI framework is especially well-suited for a derivation of kinetic theory because it provides equations of motion for the two-point function, which contains the distribution function of kinetic theory. The self-energy is decomposed into three parts in this framework. The first one being $\Sigma^{(0)}$, which is the local mean-field part adding to the effective mass (3.23) as seen later on. The other two are Σ^F and Σ^p , which are the real and imaginary contributions familiar from (3.11). The self-energy is then defined as

$$\Sigma(x, y) := 2i \frac{\delta \Gamma_2[\phi, G]}{\delta G(x, y)} =: -i \Sigma^{(0)}(x) \delta_{\mathcal{C}}(x - y) + \Sigma^F(x, y) - \frac{i}{2} \Sigma^p(x, y) \text{sgn}_{\mathcal{C}}(x^0 - y^0). \quad (3.21)$$

This self-energy sums all 1PI graphs obtained by opening a propagator line in the vacuum graphs of Γ_2 , as indicated by the derivative. The self-energy Σ as defined via Γ_2 are the sums of 1PI diagrams with two external legs with respect to the *resummed* propagator G . The "tadpole" contribution

$$\Sigma^{(0)} = \text{---}\bigcirc\text{---}$$

is singular in real space for φ^4 with one propagator $G(x, x)$. This diagram will contribute to the effective mass of the theory. Other models do not exhibit such a mean-field shift as they do not have a tadpole diagram, such as QED [29].

With the definition of the self-energy (3.21) at our disposal and by swapping the singular part to the left-hand-side (LHS), the scalar 2PI equation of motion for the propagator

(3.16) can then be written down explicitly [22], suppressing indices momentarily

$$\left[\left(\square_x + m^2 + \frac{\lambda}{6N} \phi^2(x) \right) + \Sigma^{(0)}(x) \right] G(x, y) = -i \int_{z, \mathcal{C}} \bar{\Sigma}(x, z) G(z, y) - i \delta_{\mathcal{C}}(x - y). \quad (3.22)$$

This effectively amounts to a modification of the mass term

$$m^2 \rightarrow M^2(x) = m^2 + \frac{\lambda}{6N} \phi^2(x) + \Sigma^{(0)}(x). \quad (3.23)$$

Using the decomposition into the statistical and spectral components (3.11), the 2PI equation of motion for the full propagator in (3.16) or (3.22) can be replaced by a pair of coupled evolution equations

$$[\square_x + M^2(x)] F(x, y) = - \int_{t_0}^{x^0} dz \Sigma^\rho(x, z) F(z, y) + \int_{t_0}^{y^0} dz \Sigma^F(x, z) \rho(z, y), \quad (3.24)$$

$$[\square_x + M^2(x)] \rho(x, y) = - \int_{y^0}^{x^0} dz \Sigma^\rho(x, z) \rho(z, y), \quad (3.25)$$

where we used the notation $\int_{t_1}^{t_2} dz \equiv \int_{t_1}^{t_2} dz^0 \int d^3z$ [22]. These are coupled tensorial integro-differential equations. Their structure is completely determined by causality and details of the underlying theory enter through the differential operators and self-energies, which couple the spectral function and statistical propagator to each other. The Keldysh contour results in explicit memory integrals effectively summing the causal history.

To solve (3.24) and (3.25), initial conditions for the statistical propagator have to be prescribed. The initial conditions for the spectral function are fixed by the equal-time commutation relations (3.15).

It will be necessary in the derivation of kinetic theory to reduce the structure of (3.24) and (3.25), which will be achieved by a number of assumptions collectively addressed by the *kinetic limit*.

Nonequilibrium evolution of the free spectral function

In order to understand the nonequilibrium dynamics of the spectral function ρ in comparison with the statistical two-point function F , it is instructive to consider the free field theory. With $\Sigma = 0$ and $\phi = 0$ for a spatially homogeneous system, the nonequilibrium evolution equation for the free spectral function (3.25)

$$(\partial_{x^0}^2 + \omega_{\vec{p}}^2) \rho^{(\text{free})}(x^0, y^0, |\vec{p}|) = 0, \quad (3.26)$$

with $\omega_{\vec{p}} = \sqrt{\vec{p}^2 + m^2}$ is solved after a Fourier transformation with respect to the relative time $s^0 = x^0 - y^0$ by

$$\rho^{(\text{free})}(p^0, |\vec{p}|) = i 2\pi \text{sgn}(p^0) \delta((p^0)^2 - \omega_{\vec{p}}^2). \quad (3.27)$$

In the absence of interactions and finite time effects, the spectral functions consists of delta-peaks in frequency space determined by the on-shell condition $\omega = \pm\omega_{\vec{p}}$. We can therefore obtain a particle picture by interpreting these peaks as bound particle states of energy $\omega_{\vec{p}} = \sqrt{\vec{p}^2 + m^2}$. We note that particle number is not conserved as one can convert energy into particles and back again by virtue of the relativistic dispersion relation $\omega_{\vec{p}} = \sqrt{\vec{p}^2 + m^2}$ in any relativistic QFT. Crucially, the on-shell condition is at the core of a particle picture.

Including interaction, the equilibrium spectral function will consist of a continuous spectrum of multiple peaks where each acquires a width. Therefore, speaking of particles essentially constitutes speaking about peaks in the spectral function. These peaks can now have different shapes deviating from a delta-function, corresponding to fundamental or composite particles, bound states or quasi-particles. So far, this holds true for vQFT and NeqQFT. The essential difference is that the latter also considers the real-time dynamics of the spectrum as it evolves during a collision event. For a process $A \rightarrow B$ this means that occupation of the peak characterizing species A is transported over to the spectral peak characterizing species B .

Evolution of the background field

Using the decomposition of (3.17), the equation of motion in (3.16) for the background field takes the following form for the employed model [22]

$$\left\{ \left(\square_x + m^2 + \frac{\lambda}{6N} (\phi^2(x) + F_{cc}(x, x)) \right) \delta_{ab} + \frac{\lambda}{3N} F_{ab}(x, x) \right\} \phi_b(x) = \frac{\delta\Gamma_2}{\delta\phi_a(x)}. \quad (3.28)$$

The solution of this equation requires specifying the field and its first derivative at initial time, e.g. $\phi|_{t=t_0} = \phi_0$ and $\dot{\phi}|_{t=t_0} = 0$.

3.2.6 Approximating the effective action

With the 2PI effective action our disposal (3.17), solving for dynamics analytically and also numerically requires one to make approximations to Γ_2 . The following discussion of approximation methods summarizes section 3.1 and 3.2 of [22].

A widely employed truncation method is a perturbative loop expansion of Γ_2 in the coupling constant. In contrast to perturbative treatments in vQFT, this expansion however only applies to the class of 2PI diagrams to be considered, where the propagator is already selectively resummed by virtue of the stationary principle in a 2PI loop expansion, thereby curing secularity and infrared divergences [22]. The resummation is complete to given loop order, but already contains a subset of diagrams of higher loop order. This perturbative expansion is therefore selective and already encompasses a multitude of interactions to LO in the coupling. However, even in the presence of weak couplings as for the Higgs, the dynamics of the propagator can obstruct the power counting with time hindering control over the expansion, a dynamical power counting scheme has to be devised to guarantee the validity of this expansion.

Another powerful approximation scheme is provided by the 2PI $1/N$ expansion. It is applicable to N -component scalar field theories with an $\mathcal{O}(N)$ symmetry and is based on classification of the contributions to the 2PI effective action according to their scaling with N . Particularly for the employed model, one has

$$\Gamma_2[\phi, G] = \underbrace{\Gamma_2^{LO}[\phi, G]}_{\sim N^1} + \underbrace{\Gamma_2^{NLO}[\phi, G]}_{\sim N^0} + \underbrace{\Gamma^{NNLO}[\phi, G]}_{\sim N^{-1}} + \dots$$

Importantly, this provides an expansion parameter and does not restrict to systems with small couplings or to small occupation numbers. It is an inherently nonperturbative method in the sense that an expansion in $1/N$ remains valid for large couplings [30, 31]. We will employ the former perturbative expansion scheme in 3.5 to LO in a strong-field coupling counting.

3.3 The Goldstone theorem revisited - SSB in NeqQFT

In this section, we want to discuss the process of SSB in the context of NeqQFT to provide a comparison to our treatment for vQFT in 2.3. We follow a presentation by Shen et al. [32]. This will provide us with an understanding of the rich information contained in NeqQFT, where taking the dynamical evolution of the background field into account grants us access to a more diverse distinction of the underlying physical processes.

The following discussion takes advantage of the classical intuition for a particle moving in an energy potential. This intuition has to be applied with care, since the concept of potential or kinetic energy is not at all clear out of equilibrium, especially not for strong fields, since the field is a dynamical object. For an explicit discussion around energy configurations, one would have to integrate over the local dynamics of the expectation value of the energy momentum tensor.

Consider again φ^4 theory

$$V(\varphi) = \frac{1}{2}m^2\varphi^2 + \frac{\lambda}{4!}\varphi^4, \quad (3.29)$$

where a tachyonic mass $m^2 < 0$ facilitates SSB of the classical ground state. The global vacuum configurations coincide with a double-well described by $\varphi_0 = \pm\sqrt{-3!m^2/\lambda}$. Starting from the meta-stable $\varphi_0 = 0$ minimum, the field will move towards a global minimum by virtue of its classical equation of motion if the classical approximation is valid. In the course of approaching a true ground state, the field will oscillate until it equilibrates in the minimum. For quantum theory, the corrections lead to an effective quantum potential which dominates the classical potential. Including the nonequilibrium dynamics will further introduce additional quantum fluctuations. By moving towards a global ground state, the field itself then generates quantum fluctuations which introduces a dynamical feedback effect whereby the effective potential itself is deformed, again influencing the field by a modification of its curvature. Further, these fluctuations of the field can be interpreted in the context of particle production, which we will give a full account of 3.6 after we have established the important processes of particle production.

Still, in the context of SSB, the motion towards a minimum configuration and damped oscillations around it result in an effectively irreversible energy flow from the field to the modes due to the creation of massless Goldstone bosons [24]. The contributions of the quantum corrections to the effective potential can be quantified with the energy density of the system. Quantum fluctuations modify the classical shape away from a double-well potential towards a tilted or generally deformed version of it. Depending on the initial field amplitude and the effective potential of the underlying theory, in the course of time evolution the effective potential can be either drastically modified or not at all, such that a wide range of late-time minima are possible. Crucially, depending on the initial background field amplitude, this modification leads to different late times, thermalized values $v \rightarrow \langle \phi(t) \rangle = \phi(t)$. This feedback effect then additionally modifies the resulting mass matrix (2.7). The particle masses have therefore also considered to be dynamical objects², which supports our use of a dynamical particle picture. Incorporating all orders of interaction in a resummed approach³, the increased amount of interactions results in a stronger damping of the dynamical field oscillations. The closer the field is initialized to the final late-time value, the less damping takes place, resulting in less modification of the effective potential through the feedback effect. Overall, the SSB process thereby not only depends on the dynamics of the background field but, crucially, also on the field initial conditions, possibly resulting in a large range of thermalized late-times values.

Summarizing, the difference for SSB in vQFT and NeqQFT is that the latter takes the dynamical evolution of the background field into account, thereby introducing a self-consistent feedback effect on the possible dynamics of the field. Subsequently, this leads to a dynamical modification of particle masses, facilitating a dynamical emergent particle picture. Considering a wide class of initial conditions, a plethora of late-time values not coinciding with the vQFT value $\phi(t \rightarrow +\infty) \neq v$ are possible.

3.4 Scalar strong-field kinetic theory

Making a set of assumptions about the dynamics of the system itself, collectively addressed in the *kinetic limit*, the 2PI equation of motion of the statistical propagator (3.24) can be converted into Boltzmann-like kinetic equation

$$\frac{\partial f(t, \vec{p})}{\partial t} = C[f](t, \vec{p}), \quad (3.30)$$

where the time evolution of the on-shell particle distribution function $f(t, \vec{p})$ is governed by all possible scattering processes between the constituents of the theory as contained in the collision functional $C[f]$. The way to arrive at kinetic theory is completely self-contained in the framework of NeqQFT, where the kinetic limit provides the necessary

²We note here that the validity of Goldstone's theorem in the 2PI framework has been proven by Berges et al. in [31].

³This was done in [32] by employing NLO $1/N$ resummed kinetic theory.

reduction of information to arrive at an effective description for nonequilibrium many-body dynamics. The difference to ad hoc kinetic theory is that we aim to arrive at a kinetic theory self-consistently within the 2PI framework which is applicable to the strong-field regime relevant for Higgsproduction.

We stress this point, that traditional zero-field kinetic theory is *not* able to include a dynamical and inhomogeneous background field. Our aim is to develop such a kinetic theory which couples to the dynamic of the background field by a self-consistent reduction procedure starting from the 2PI equations of motion.

Kinetic theory facilitates a dynamical description of particle occupation numbers by tracking the dynamics of the distribution function $f(X, \vec{p})$. For a spectral function describing a continuum of states, the particle picture is not applicable and such a description is ill-posed due to the corresponding off-shell transport of occupations. This is the realm described by the more general transport theory [22]. The distinction between transport and kinetic theory is that the former deals with off-shell observables whilst the latter facilitates a particle picture by considering on-shell observables by virtue of a free (for our purposes strong-field) spectral function with delta-shaped peak structure in frequency space. We will not make this distinction any more in the following and simply address the resulting equations as kinetic.

In contrast to the asymptotic state formalism of vQFT, what kinetic theory is able to achieve is retaining the information contained in real-time dynamics. At the core of kinetic theory are three important assumptions coined the kinetic limit, explicitly the Kadanoff-Baym ansatz, the late-time limit and the gradient expansion. The latter allows for a reduction of the rich information contained in the 2PI equations of motion (3.24), (3.25) and (3.28) by assuming a separation of scales between the collision scale and the scale of propagating degrees of freedom. Such an assumption allows one to decouple the interplay between spectral and statistical dynamics. As we will see shortly, it does however not suffice to decouple neither spectral nor statistical dynamics from background field dynamics since we are considering the strong-field regime. In contrast to the infinite past to infinite future framework of vQFT, kinetic theory only imposes a late-time limit allowing one to track infinite past to real time dynamics. This will enable us to investigate particle production by granting us access to local, real-time observables such as the particle number $N(t)$. Possible treatments include neglecting the collision term and thereby thermalization as a whole, where the resulting Vlasov-equation still provides considerable insight. This approach will later on yield a collisionless particle production mechanism at $\mathcal{O}(\lambda^0)$ facilitated by a drift term. For our purposes, we are in particular interested in the collision functional since it encodes $\mathcal{O}(\lambda)$ particle production through inelastic scatterings in the language of local scattering amplitudes and decay widths, which is therefore especially suitable for a comparison with results from vQFT.

In the following, we will begin by going through the assumptions of the kinetic limit. Subsequently, these assumptions are applied to the 2PI equations of motion for the statistical (3.24) and spectral function (3.25) as well as for the background field (3.28). This will result in a closed kinetic system for the strong-field regime, respectively the

strong-field equation (3.47), the strong-field spectral function (3.48) and the off-shell equation for the statistical propagator (3.51). Finally, combining the latter two will yield the Boltzmann-like equation for the on-shell distribution function (3.57), which we will call the kinetic equation in the following. Subsequently, these equations are specified to leading order in the strong-field coupling and collected in (3.84).

3.4.1 Kadanoff-Baym Ansatz

Thermalization eventually leads to thermal equilibrium, which is characterized by the emergence of a temperature and a canonical density matrix $\rho \propto e^{-\beta H}$. This reduction of degrees of freedom in terms of the density of states and in terms of an averaging process over the microscopic momenta of the theory $T \sim p$ leads to the emergence of the so-called *fluctuation-dissipation relation* (FDR), which relates the statistical and spectral function by encoding the statistical aspects in terms of the occupation number distribution $f_\beta(\omega)$ (e.g. for bosons)

$$F^{(eq)}(\omega, \vec{p}) = -i \left[\frac{1}{2} + f_\beta(\omega) \right] \rho^{(eq)}(\omega, \vec{p}), \quad (3.31)$$

where $f_\beta(\omega) = (e^{\beta\omega} - 1)^{-1}$ denotes the thermal Bose-Einstein (BE) distribution function. The form of the BE distribution function conveys what we have already discussed in the previous sections, namely that, in thermal equilibrium, the system becomes homogeneous and isotropic. Translation invariance under the four-momentum is restored.

Note that systems without interactions can not thermalize. An FDR does not exist out of equilibrium. They emerge by virtue of a huge reduction of complexity leading up to the characterisation of the system in terms of thermal equilibrium correlation function. Another general relation exists in vacuum, where $f_\beta(\omega) \equiv 0$ such that the spectral and statistical function coincide up to a normalization factor [22].

To relate the out-of-equilibrium spectral and statistical dynamics, one can however make an off-shell Kadanoff-Baym ansatz (KBA) for a generalized distribution function. Originally defined on-shell in [33] and discussed for our purposes in [21], it entails in Wigner space

$$F(X, p) = -i \left[\frac{1}{2} + f(X, p) \right] \rho(X, p), \quad (3.32)$$

which will serve us to define the effective occupation number distribution f for an emergent kinetic particle picture (3.52) by restricting the distribution function to an effective and dynamical mass shell through the strong-field spectral function. The thermal interpretation from FDR as $f(X, p)$ encoding the occupation densities of Fourier modes is thereby retained far-from-equilibrium through the KBA [29].

3.4.2 Late-time limit

Similar to the asymptotic state formalism in vQFT, we consider well-separated time scales to provide the validity of a separation of scales in a subsequent kinetic gradient

expansion. This assumption explicitly consists of considering observation times long after the initial time $t \gg t_0$, or effectively $t_0 \rightarrow -\infty$. We will therefore consider an asymptotic past to real time dynamic evolution which is exactly the regime we are interested in since we can test the dynamics of the past before thermalization has taken place, i.e. before we reach the asymptotic future.

Technically, in conjunction with a subsequent kinetic gradient expansion, the late-time limit will guarantee the usage of infinite-time Wigner transformations and reduce the memory integrals in the 2PI equations of motion (3.24) and (3.25) to local expressions in time.

3.4.3 Kinetic gradient expansion

A final essential approximation is that a gradient expansion is employed. This means that only terms up to a specific order in the number of derivatives with respect to the centre coordinates X^μ and powers of the relative coordinates s^μ , defined as

$$X^\mu = \frac{x^\mu + y^\mu}{2}, \quad s^\mu = x^\mu - y^\mu$$

are kept. These variables correspond to the position and momentum variable in Wigner space. The associated expansion parameter is then in coordinate space and Wigner space respectively

$$(s \cdot \partial_X) \ll 1, \quad (\partial_p \cdot \partial_X)^n g(X, p) \ll 1, \quad (3.33)$$

where the latter notation is supposed to indicate a gradient expansion to n -th order for the two-point function $g(X, p)$ in Wigner space. This assumption amounts to a slow variation of the two-point function with X and is essential for the derivation of a Boltzmann-like kinetic theory. By employing the gradient expansion, one makes an implicit assumption about a separation of scales between the collision scale and the propagation scale. This is the assumption common with traditional zero-field kinetic theory, where the regime of validity suffices as long as the duration of scattering is far smaller than the mean free time of a particle. Effectively, this entails ignoring quantum effects during propagation where interactions are localized around scattering events [29].

When dealing with a strong background field, one has to distinguish between a gradient expansion in propagator-gradients (ρ or F) and one in field-gradients. However, keeping track of these three different expansion parameters becomes cumbersome very quickly and physical intuition is lost. To alleviate this, we will collect these two systematic expansions, the gradient expansion and the coupling expansion, in one systematic *strong-field coupling* expansion. To this end, we assume that the counting in gradients and the counting in the coupling is related via

$$(\partial_p \cdot \partial_X) \sim \lambda. \quad (3.34)$$

The explicit form of this relation is chosen such as to be valid for the strong-field regime which can describe far-from-equilibrium phenomena⁴. This will allow us to not distinguish between the gradient expansion (in either propagator- or field-gradients) and the coupling expansion, we just resort to one strong-field coupling counting. Importantly, we stress that this is an assumption by which we limit the possible experimental set-up, all our equations can however equally be derived by consistently expanding to LO in propagator-gradients, NLO in field-gradients and LO in the coupling under the strong-field counting $\phi \sim 1/\sqrt{\lambda}$. We only resort to this strong-field coupling counting for transparency into the underlying physical processes.

3.4.4 Scalar kinetic theory for the strong-field regime

Having listed the assumptions for a sufficiently reduced effective description, we can employ these to uncover a kinetic framework suitable for describing nonequilibrium strong-field dynamics. Such a description is expected to be reasonable for comparably smooth time evolution, with the occupation numbers changing much slower compared to the oscillations of the momentum modes.

It is convenient to Wigner transform the two-point functions, which is just a Fourier transformation with respect to the relative coordinates. For example

$$F(X, p) = \int_s e^{ips} F(X + \frac{s}{2}, X - \frac{s}{2}), \quad (3.35)$$

$$\rho(X, p) = -i \int_s e^{ips} \rho(X + \frac{s}{2}, X - \frac{s}{2}), \quad (3.36)$$

where one conventionally includes a factor i to have $i\rho(X, p^0, \vec{p})$ real.

A gradient expansion of two-point functions is achieved by the identity [22]

$$\int d^4s e^{ips} (f \star g)(X + \frac{s}{2}, X - \frac{s}{2}) = \exp \left\{ \frac{i}{2} \left[\frac{\partial}{\partial p_\sigma} \frac{\partial}{\partial X'^\sigma} - \frac{\partial}{\partial p'_\sigma} \frac{\partial}{\partial X^\sigma} \right] \right\} f(X, p) g(X', p')|_{X'=X, p'=p}, \quad (3.37)$$

where the convolution reads

$$(f \star g)(x, y) = \int_z f(x, z) g(z, y). \quad (3.38)$$

Expansion of the exponential corresponds to a gradient expansion in Wigner space $(\partial_p \cdot \partial_X)$, which amounts to a strong-field coupling expansion through the strong-field counting rule (3.34).

To derive a kinetic system in Wigner space, one considers differences of the 2PI equations of motion (3.24), (3.25) and (3.28), where the detailed procedure for zero-field kinetic theory can for example be found in [22]. Using the chain rule, one obtains

$$\square_x - \square_y = 2 \frac{\partial}{\partial s_\sigma} \frac{\partial}{\partial X^\sigma}. \quad (3.39)$$

⁴Later on in 3.4.6, we will have to adjust this counting rule for the weak-field limit which is close to equilibrium.

Concerning the differences $M^2(x) - M^2(y)$, for the strong-field regime the effective mass

$$M^2(x) = m^2 + \frac{\lambda}{6}\phi^2(x) + \Sigma^{(0)}(x). \quad (3.40)$$

contains a $\mathcal{O}(\lambda^0)$ contribution ⁵

$$M^2 \supseteq \frac{\lambda}{6}\phi^2 \sim \mathcal{O}(\lambda^0).$$

$\partial_X M^2 \partial_p$ is NLO in the field-gradient expansion, which is why it is neglected in traditional zero-field derivations of kinetic theory. For the strong-field regime, the gradient of the effective mass however is $\mathcal{O}(\lambda)$ in the strong-field coupling as

$$\partial_X M^2 \cdot \partial_p \sim \lambda(\partial_X \phi^2 \cdot \partial_p) \sim \mathcal{O}(\lambda^2/\lambda) = \mathcal{O}(\lambda). \quad (3.41)$$

If we want to be complete at LO in the strong-field coupling, then we have to take this contribution by the effective mass into account. The NLO gradient expansion of the effective mass differences then yields the LO strong-field coupling contribution

$$M^2(X + \frac{s}{2}) - M^2(X - \frac{s}{2}) \simeq s^\sigma \frac{\partial M^2(X)}{\partial X^\sigma}. \quad (3.42)$$

This term conventionally facilitates an effective force description $\mathcal{F}_\mu \frac{\partial}{\partial p^\mu}$ in kinetic theory⁶, which we will isolate explicitly in the following around (3.56). For now, we already stress that the effective mass serves as an effective potential, where we can define a force as the gradient of this effective potential as

$$\mathcal{F}_\mu(X) = \frac{\partial M^2(X)}{\partial X^\mu}. \quad (3.43)$$

As we will later on see 3.5, understanding the drift term effectively amounts to understanding how fluctuations of the background field are translated into the production of particles.

Altogether, the LHS of the equations of motion of the two-point functions at LO in the strong-field coupling reads

$$\begin{aligned} & \int d^4s e^{ip_\mu s^\mu} \left[2 \frac{\partial}{\partial s_\sigma} \frac{\partial}{\partial X^\sigma} + s^\sigma \frac{\partial M^2(X)}{\partial X^\sigma} \right] f(X + \frac{s}{2}, X - \frac{s}{2}) \\ &= -i \left[2p^\mu \frac{\partial}{\partial X^\mu} + \frac{\partial M^2(X)}{\partial X^\mu} \frac{\partial}{\partial p_\mu} \right] f(X, p). \end{aligned} \quad (3.44)$$

The right-hand-side (RHS) is transformed in a similar fashion by virtue of the convolution identity (3.37), the explicit form is given later on for the specific two-point functions.

⁵At least for initial time, a discussion of strong-field power counting requires to take the background field dynamics explicitly into account.

⁶In QED, this term is LO in the gradient expansion and leads to the Lorentz force equation [29].

Strong-field equation for the background field

Acquiring a self-consistent set of equations for strong-field scalar kinetic theory is achieved by taking the 2PI equation of motion of the background field (3.28) into account. The necessary transformation into Wigner space requires a technical manipulation since one can not Wigner transform one-point functions. To this end, we employ the following disconnected two point function

$$\Phi(x, y) := \phi(x)\phi(y), \quad (3.45)$$

which will suffice to circumvent these obstructions to a self-consistent treatment to LO in the strong-coupling of the background field within φ^4 theory. Φ is symmetric in coordinate and Wigner space

$$\Phi(x, y) = \Phi(y, x), \quad \Phi(X, p) = \Phi(X, -p). \quad (3.46)$$

Making use of the fact that

$$\phi(y)\square_x\phi(x) = \square_x[\phi(x)\phi(y)] \equiv \square_x\Phi(x, y),$$

we can derive the strong-field equation by following the procedure detailed above

$$\begin{aligned} \int_s e^{ips} [\square_x - \square_y + M^2(x) - M^2(y)] \Phi(x, y) \\ = \int_s e^{ips} \left[\frac{\delta\Gamma_2}{\delta\phi(x)} \phi(y) - \frac{\delta\Gamma_2}{\delta\phi(y)} \phi(x) \right], \end{aligned} \quad (3.47)$$

where a subsequent expansion to LO in the strong-field coupling is employed with the convolution identity (3.37) upon having the explicit self-energies at given coupling order at our disposal.

Strong-field equation for the spectral function

Performing the manipulations for the 2PI equation of motion of the spectral function (3.25), the RHS cancels to LO in the gradient expansion and we obtain the strong-field spectral equation to LO in propagator gradients and NLO in field-gradients as⁷

$$-i \left[2p^\mu \frac{\partial}{\partial X^\mu} + \mathcal{F}_\mu(X) \frac{\partial}{\partial p_\mu} \right] \rho(X, p) = 0 + \mathcal{O}((\partial_p \cdot \partial_X)^1 H) + \mathcal{O}((\partial_p \cdot \partial_X)^2 \Phi), \quad (3.48)$$

where $H \in \{F, \rho\}$. We observe that the gradient expansion facilitates a decoupling of spectral from statistical dynamics as conventional for kinetic theory [34], where an implicit coupling to the background field however only enters through the drift term.

⁷We give here the explicit order in the gradient expansion to stress that no loop expansion has been employed so far. We will collect these systematic approximations in the strong-field coupling expansion upon analysing specific 2PI diagrams.

The Wigner space solution of this equation of motion is given by the strong-field spectral function

$$\rho^{(\text{strong})}(X, p^0, \vec{p}) = -i2\pi \text{sgn}(p^0) \delta((p^0)^2 - \omega_{\vec{p}}^2[\Phi](X)) \quad (3.49)$$

with the field-dependent dispersion relation $\omega_{\vec{p}}^2[\Phi](t) = \vec{p}^2 + M^2[\Phi](t)$.

Notice that (3.49) corresponds to the free spectral function (3.27) with a dynamical peak position. The field-dependent dispersion relation effectively couples the fluctuations generated by the strong background field into the spectral dynamics already at LO in the strong-field coupling. We stress here that this coupling to field dynamics is absent in traditional zero-field derivations, where the spectral function completely decouples and takes on the free field form (3.27).

Summarizing, the spectral kinetic equation has to be modified in the presence of a strong-field, because the effective mass contains a contribution which is $\mathcal{O}(\lambda^0)$ in the strong-field coupling counting. This contribution effectively couples the background field to spectral dynamics, leading to a dynamical peak position in the resulting spectral function which amounts to a mass-shift.

We note here that gap-less modes are not consistent with the equation of motion (3.48) upon employing the strong-field solution (3.49), since

$$\begin{aligned} & -i \left[2p^\mu \frac{\partial}{\partial X^\mu} + \mathcal{F}_\mu(X) \frac{\partial}{\partial p_\mu} \right] \rho^{(\text{strong})}(X, p^0, \vec{p}) \\ &= -i2\pi \frac{\partial M^2(X)}{\partial X^0} \frac{\delta^{(1)}(p^0 - \omega_{\vec{p}}) \delta^{(1)}(p^0)}{p^0} = \begin{cases} 0 & \text{if } \omega_{\vec{p}}[\phi](X) \neq 0 \\ -i2\pi \mathcal{F}_0(X) \frac{\delta^{(1)}(\omega_{\vec{p}})}{\omega_{\vec{p}}} & \text{if } \omega_{\vec{p}}[\phi](X) = 0, \end{cases} \end{aligned} \quad (3.50)$$

where the equation (3.48) is solved by (3.49) if the product of delta functions has vanishing support, i.e. where the field-dependent dispersion relation is non-vanishing. This is elaborated on further around (3.97).

Strong-field equation for the statistical propagator and strong-field kinetic equation

Similarly, one transforms the 2PI equation of motion of the statistical propagator (3.25), where we leave the interactions unspecified for now. Therefore, the resulting statistical equation to LO in propagator gradients and NLO in field-gradients reads

$$\begin{aligned} & -i \left[2p^\mu \frac{\partial}{\partial X^\mu} + \mathcal{F}_\mu(X) \frac{\partial}{\partial p_\mu} \right] F(X, p) = \Sigma^F(X, p) \rho(X, p) - \Sigma^p(X, p) F(X, p) \\ & \quad + \mathcal{O}((\partial_p \cdot \partial_X)^1 H) + \mathcal{O}((\partial_p \cdot \partial_X)^2 \Phi). \end{aligned} \quad (3.51)$$

We are now in a position to rephrase the statistical equation into a Boltzmann-like form. To this end, we find an effective occupation number distribution via the KBA (3.32) by

employing the strong-field spectral function (3.49)

$$f(X, \vec{p}) := i \int_0^\infty \frac{dp^0}{2\pi} 2p^0 \rho(X, p) f(X, p) = \int_0^\infty dp^0 \delta^{(1)}(p^0 - \omega_{\vec{p}}) f(X, p). \quad (3.52)$$

For the free-field form of the spectral function (3.27), this definition gives the particle number which is on-shell with respect to $p^2 = m^2$. For our purposes, we have to employ the strong-field spectral function (3.49) with on-shell condition $p^2 = M^2$ here and in the following for a self-consistent analysis. Plugging (3.52) into (3.51) leads to⁸

$$\begin{aligned} \left[\frac{\partial}{\partial X^0} + \frac{p_i}{\omega_{\vec{p}}} \frac{\partial}{\partial X^i} \right] f(X, \omega_{\vec{p}}, \vec{p}) + \mathcal{F}_\mu(X) \frac{1}{2\omega_{\vec{p}}} \frac{\partial f(X, p)}{\partial p_\mu} \Big|_{p^0=\omega_{\vec{p}}} \\ = C[f](X, \vec{p}) + \mathcal{O}((\partial_p \cdot \partial_X)^1 H) + \mathcal{O}((\partial_p \cdot \partial_X)^2 \Phi), \end{aligned} \quad (3.53)$$

where the collision functional to LO in propagator-gradients is given by

$$C[f](X, \vec{p}) = i \int_0^\infty \frac{dp^0}{2\pi} \left[\Sigma^\rho(X, p) F(X, p) - \Sigma^F(X, p) \rho(X, p) \right] + \mathcal{O}((\partial_p \cdot \partial_X)^1 H). \quad (3.54)$$

We can turn this equation into a Boltzmann-like form by re-writing the energy derivative as follows

$$\begin{aligned} \frac{\partial f(X, p)}{\partial p^0} \Big|_{p^0=\omega_{\vec{p}}} &= \frac{\partial p_i}{\partial \omega_{\vec{p}}} \frac{\partial}{\partial p_i} f(X, \omega_{\vec{p}}, \vec{p}) = \frac{1}{v_{i,\text{group}}} \frac{\partial}{\partial p_i} f(X, \omega_{\vec{p}}, \vec{p}) \\ \text{with } v_{i,\text{group}} &:= \frac{\partial \omega_{\vec{p}}}{\partial p^i} = \frac{p_i}{\omega_{\vec{p}}} = \left(\frac{\partial p^i}{\partial \omega_{\vec{p}}} \right)^{-1}, \end{aligned} \quad (3.55)$$

where the last inequality only holds if $\omega_{\vec{p}} = \sqrt{\sum_{j=1}^3 p_j^2 + M^2}$ is invertible. Further, we can define an effective force by grouping the gradient force $\mathcal{F}^\mu(X) = \partial_X^\mu M^2(X)$,

$$\mathcal{F}_i^{\text{eff}}(X, \omega_{\vec{p}}, \vec{p}) := \frac{1}{2\omega_{\vec{p}}} \left[\frac{1}{v_{i,\text{group}}} \mathcal{F}_0(X) + \mathcal{F}_i(X) \right]. \quad (3.56)$$

The Boltzmann-like strong-field kinetic equation at LO in propagator-gradients and NLO in field-gradients then becomes

$$\begin{aligned} \frac{d}{dt} f(X, \omega_{\vec{p}}, \vec{p}) &= \left[\frac{\partial}{\partial X^0} + v_{i,\text{group}} \frac{\partial}{\partial X^i} + \mathcal{F}_i^{\text{eff}}(X, \omega_{\vec{p}}, \vec{p}) \frac{\partial}{\partial p_i} \right] f(X, \omega_{\vec{p}}, \vec{p}) \\ &= C[f](X, \omega_{\vec{p}}, \vec{p}) + \mathcal{O}((\partial_p \cdot \partial_X)^1 H) + \mathcal{O}((\partial_p \cdot \partial_X)^2 \Phi). \end{aligned} \quad (3.57)$$

As we will discuss in more detail in the section on particle production 3.5, we already observe that the one-loop mean-field terms incorporate a collisionless change of particle number by coupling distribution functions to the mean-fields without self-interactions.

⁸We comment here that this derivation involves a caveat of when to employ the on-shell condition with respect to the strong-field spectral function (3.49) in the context of gap-less modes (3.50). We will elaborate on this further in a section on collisionless particle production in 3.5.1.

We observe explicitly that the full drift term

$$\left[\frac{\partial}{\partial X^0} + v_{i,\text{group}} \frac{\partial}{\partial X_i} + \mathcal{F}_i^{\text{eff}}(X, \omega_{\vec{p}}, \vec{p}) \frac{\partial}{\partial p_i} \right] f(X, \omega_{\vec{p}}, \vec{p}) \quad (3.58)$$

facilitates a change in occupation numbers by coupling the fluctuations of the background field contained in the effective force $\mathcal{F}_i^{\text{eff}}$ to spectral and statistical dynamics. For completeness, we will also present the kinetic equation for a spatially homogeneous system with $X^0 \equiv t$. Spatial gradients will vanish and the effective force becomes

$$\mathcal{F}_i^{\text{eff}}(t, \vec{p}) = \frac{1}{2p^i} \mathcal{F}_0(t) = \frac{1}{2p^i} \partial_t M^2(t). \quad (3.59)$$

Suppressing the globally fixed energy label $p^0 = \omega_{\vec{p}} = \sqrt{\vec{p}^2 + M^2[\phi](t)}$ for notational ease, the strong-field kinetic equation at LO in propagator gradients and NLO in field-gradients becomes

$$\left[\frac{\partial}{\partial t} + \mathcal{F}_i^{\text{eff}}(t, \vec{p}) \frac{\partial}{\partial p_i} \right] f(t, \vec{p}) = C[f](t, \vec{p}) + \mathcal{O}((\partial_p \cdot \partial_X)^1 H) + \mathcal{O}((\partial_p \cdot \partial_X)^2 \Phi). \quad (3.60)$$

The Boltzmann-like kinetic equation (3.57) will exhibit the usual gain-loss structure for the collision functional upon inserting expressions for the self-energies and re-expressing the propagators in terms of distribution functions. After a sufficient amount of time has passed, allowing for interactions to equilibrate the system, the collision term will vanish due to detailed balance as the particle distribution function approaches a Bose-Einstein form. By dropping memory integrals through the late-time limit, phase space information is discarded in the course of the time evolution rendering the process irreversible. Therefore, an irreversible evolution takes place, thereby singling out an arrow of time.

3.4.5 Scalar strong-field kinetic theory at leading order in the coupling

We will now derive an explicit kinetic system for the strong-field regime to leading order in the strong-field coupling counting.

Interactions at leading order in the coupling

We will begin at two loops, which is of linear order in the coupling for strong fields⁹. Diagrammatically, interactions consist of propagator lines connecting to either the effective three vertex or the four vertex, respectively

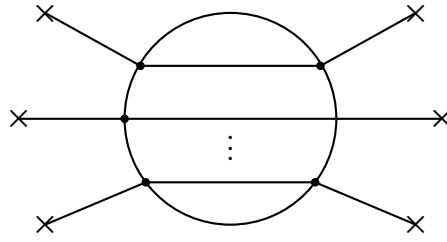
$$\begin{array}{c} \diagup \\ \bullet \\ \diagdown \end{array} \begin{array}{c} \diagup \\ \bullet \\ \diagdown \end{array} = \lambda \int_{x, \mathcal{C}} \phi(x), \quad \begin{array}{c} \diagup \\ \bullet \\ \diagdown \end{array} \begin{array}{c} \diagup \\ \bullet \\ \diagdown \end{array} = \lambda \int_{x, \mathcal{C}'} \quad (3.61)$$

⁹Power counting of the loop expansion involves subtleties as it depends on the initial conditions of the system at hand. Specifying our set-up to strong fields, we can fix a regime for the analysis.

where the insertion is meant to indicate the presence of a background field. Since we are considering the strong-field regime, one has to take the strong-field power counting of the background field into account when quantifying the dominant or sub-dominant contributions in an interaction. Importantly, processes usually suppressed by higher powers in the coupling can now become comparable if they contain factors of the background field, i.e.

$$\mathcal{O}(\Phi^n \lambda^m) \sim \mathcal{O}(\lambda^{m-n}), \quad (3.62)$$

at least initially. Therefore, an n -loop diagram involving m background fields is perturbatively comparable to a $(n - m)$ -loop diagram in the strong-field regime, pictorially we therefore have to consider higher-order strong-field diagrams for example of the form

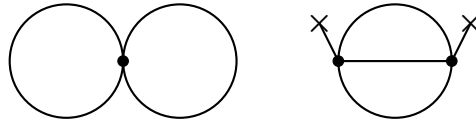


This observation requires us to take all contributions including the background field to a given order in the coupling into account, effectively amounting to consistently performing the strong-field coupling. We stress here that this only changes the ordering of diagrams, the strong-field coupling expansion is well-defined. Furthermore, the validity of the loop expansion is constrained to the regime of non-classical occupation numbers

$$F^2 \ll \frac{1}{\lambda^2}, \quad (3.63)$$

otherwise an expansion of the diagrams in the coupling becomes intractable as every diagram is $\mathcal{O}(\lambda^0)$. For occupations exceeding this condition one would have to resort to classical statistical field theory or the $1/N$ expansion [22].

At linear order in the strong-field coupling $\mathcal{O}(\lambda)$, we have to consider the diagrams



These diagrams correspond to

$$\Gamma_2^{(2-\text{loop})}[\phi, G] = \Gamma_2^{(2a)}[G] + \Gamma_2^{(2b)}[\phi, G],$$

where the field-independent contribution is

$$\Gamma_2^{(2a)}[G] = -\frac{\lambda}{8} \int_{x, \mathcal{C}} G^2(x, x). \quad (3.64)$$

The field-dependent contribution to LO in the strong-field coupling is given by

$$\Gamma_2^{(2b)}[\phi, G] = i \frac{\lambda^2}{12} \int_{xy, \mathcal{C}} \phi(x) G^3(x, y) \phi(y). \quad (3.65)$$

With (3.21), the contributions to the self-energy are identified to be

$$\begin{aligned} \Sigma(x, y) &= \Sigma^{(2a)}(x, y) + \Sigma^{(2b)}(x, y) \\ &= -i \frac{\lambda}{2} G(x, x) \delta_{\mathcal{C}}(x - y) - \frac{\lambda^2}{2} G^2(x, y) \phi(x) \phi(y) \end{aligned} \quad (3.66)$$

which decomposes to be

$$\begin{aligned} \Sigma^{(0)}(x) &= \frac{\lambda}{2} F(x, x) \\ \Sigma^{\rho}(x, y) &= -\lambda^2 F(x, y) \rho(x, y) \phi(x) \phi(y) \\ \Sigma^F(x, y) &= -\frac{\lambda^2}{2} \left[F^2(x, y) - \frac{1}{4} \rho^2(x, y) \right] \phi(x) \phi(y). \end{aligned} \quad (3.67)$$

$\Sigma^{(0)}$ is taken into account as a dynamical mass shift in the effective mass (3.40), at LO in the coupling for the strong-field regime we therefore have

$$M^2(x) = m^2 + \frac{\lambda}{2} \left[\frac{1}{3} \phi^2(x) + F(x, x) \right]. \quad (3.68)$$

From (3.65), we can derive the RHS of the field equation of motion (3.28) to read

$$\frac{\delta \Gamma^{(2b)}[\phi, G]}{\delta \phi(x)} = i \frac{\lambda^2}{6} \int_{y, \mathcal{C}} G^3(x, y) \phi(y). \quad (3.69)$$

With the explicit form of interactions at our disposal, we can now proceed to formulate a kinetic system for the strong-field regime to leading order in the coupling.

Scalar strong-field equation at leading order in the coupling

We will now explicitly write down the strong-field equation (3.47) to leading order in the strong-field coupling. For this endeavour, we will make the time-component with respect to the Keldysh contour explicit. This can be achieved by introducing so-called *Wightmann functions*. Using the decomposition of the propagator (3.11), one finds that the Wightman functions for having x^0 or y^0 on \mathcal{C}^+ or \mathcal{C}^- respectively, read

$$\begin{aligned} G^{+-}(x, y) &= F(x, y) - \frac{i}{2} \rho(x, y), \\ G^{-+}(x, y) &= F(x, y) + \frac{i}{2} \rho(x, y). \end{aligned} \quad (3.70)$$

Employing the KBA (3.32), (3.70) reads in Wigner space

$$\begin{aligned} G^{+-}(X, p) &= -i [f(X, p) + 1] \rho(X, p), \\ G^{-+}(X, p) &= -if(X, p) \rho(X, p), \end{aligned} \quad (3.71)$$

which encodes the gain-loss structure of Boltzmann equations via Bose-enhancement. Note that $+-$ implies outgoing and $-+$ ingoing particles.

At LO in the strong-field coupling counting, the interactions contributing to the field evolution equation (3.47) are given by (3.69). Explicitly splitting the time integral with respect to the Keldysh contour to employ the Wightmann functions, we can define the following object

$$\int_{z, \mathcal{C}} G^3(x, z) = \int d^3z \int_{t_0}^{x^0} dz^0 \underbrace{\left\{ \left[G^{+-}(x, z) \right]^3 - \left[G^{-+}(x, z) \right]^3 \right\}}_{=: \mathcal{G}(x, z)} \quad (3.72)$$

which is antisymmetric by virtue of

$$\mathcal{G}(x, z) = -\mathcal{G}(z, x) \quad \Leftarrow \quad G^{-+}(x, y) = G^{+-}(y, x). \quad (3.73)$$

Due to this antisymmetry, one can immediately define retarded and advanced functions¹⁰

$$\mathcal{G}_R(x, z) := \theta(x^0 - z^0) \mathcal{G}(x, z), \quad \mathcal{G}_A(x, z) := -\theta(z^0 - x^0) \mathcal{G}(x, z). \quad (3.74)$$

This allows for a solution via the convolution identity (3.37) as

$$\begin{aligned} & \int d^4s e^{ip \cdot s} \left[\frac{\delta \Gamma_2}{\delta \phi(x)} \phi(y) - \frac{\delta \Gamma_2}{\delta \phi(y)} \phi(x) \right] \\ &= i \frac{\lambda^2}{6} \int d^4s e^{ip \cdot s} \int_{\mathbb{R}^4} d^4z \theta(z^0 - t_0) [\mathcal{G}_R(x, z) \Phi(z, y) - \mathcal{G}_A(z, y) \Phi(x, z)] \\ &= i \frac{\lambda^2}{6} \Phi(X, p) \mathcal{G}(X, p) + \mathcal{O}(\lambda^2), \end{aligned}$$

where the late-time limit destroys the memory of the integral $\theta(z^0 - t_0) \rightarrow 1$ and already the Poisson-Bracket

$$\{\mathcal{G}(X, p), \Phi(X, p)\}_{\text{P.B.}} = \frac{\partial \mathcal{G}(X, p)}{\partial p_\mu} \frac{\partial \Phi(X, p)}{\partial X^\mu} - \frac{\partial \Phi(X, p)}{\partial p_\mu} \frac{\partial \mathcal{G}(X, p)}{\partial X^\mu} \quad (3.75)$$

drops out since it is NLO in the strong-field power counting as

$$\lambda^2 \{\mathcal{G}(X, p), \Phi(X, p)\}_{\text{P.B.}} \sim \mathcal{O}(\lambda^2). \quad (3.76)$$

¹⁰Conventionally, these functions are defined with respect to the antisymmetric ρ component of the two-point function. Since \mathcal{G} is antisymmetric, we can conclude that $\mathcal{G}^\rho(x, y) \equiv \mathcal{G}(x, y)$.

Specifying the Wightmann function in Wigner space (3.71), the collision kernel exhibits a gain-loss structure

$$\begin{aligned}\mathcal{G}(X, p) &= \int d^4s e^{ips} \mathcal{G}(X + \frac{s}{2}, X - \frac{s}{2}) \\ &= i \int \frac{d^4k_1}{(2\pi)^4} \frac{d^4k_2}{(2\pi)^4} \frac{d^4k_3}{(2\pi)^4} (2\pi)^4 \delta^{(4)}(k_1 + k_2 + k_3 - p) \rho(X, k_1) \rho(X, k_2) \rho(X, k_3) \\ &\quad \{ [f(X, k_1) + 1][f(X, k_2) + 1][f(X, k_3) + 1] - f(X, k_1)f(X, k_2)f(X, k_3) \}.\end{aligned}$$

Explicitly considering the strong-field spectral function (3.49), we can split the frequency integrals onto the positive energy domain $k_i^0 \in (-\infty, \infty) \mapsto k_i^0 \in (0, \infty)$ and make use of the symmetry property

$$f(X, -k) = -[f(X, k) + 1]. \quad (3.77)$$

Executing the frequency integrals and relabelling under the momentum integrals, the strong-field equation at LO in the strong-field coupling becomes

$$\begin{aligned}&\left[2p^\mu \frac{\partial}{\partial X^\mu} + \mathcal{F}_\mu[\Phi](X) \frac{\partial}{\partial p_\mu} \right] \Phi(X, p) = -\frac{\lambda^2}{6} \Phi(X, p) \mathcal{G}[\Phi, f](X, p) + \mathcal{O}(\lambda^2) \quad (3.78) \\ &= \frac{\lambda^2}{6} \Phi(X, p) \int_{\mathbb{R}^9} \frac{d^3k_1 d^3k_2 d^3k_3}{(2\pi)^9 2\omega_{\vec{k}_1}[\Phi](X) 2\omega_{\vec{k}_2}[\Phi](X) 2\omega_{\vec{k}_3}[\Phi](X)} (2\pi)^4 \\ &\quad \left\{ 3 \left[\delta^{(3)}(\vec{k}_2 + \vec{k}_3 - \vec{k}_1 - \vec{p}) \delta^{(0)}(\omega_{\vec{k}_2} + \omega_{\vec{k}_3} - \omega_{\vec{k}_1} - p^0) \right. \right. \\ &\quad \left. \left. + \delta^{(3)}(\vec{k}_2 + \vec{k}_3 + \vec{p} - \vec{k}_1) \delta^{(0)}(\omega_{\vec{k}_2} + \omega_{\vec{k}_3} + p^0 - \omega_{\vec{k}_1}) \right] \right. \\ &\quad \times \left[[f(X, \vec{k}_1) + 1] f(X, \vec{k}_2) f(X, \vec{k}_3) - f(X, \vec{k}_1) [f(X, \vec{k}_2) + 1] [f(X, \vec{k}_3) + 1] \right] \\ &\quad + \left[\delta^{(3)}(\vec{k}_1 + \vec{k}_2 + \vec{k}_3 - \vec{p}) \delta^{(1)}(\omega_{\vec{k}_1} + \omega_{\vec{k}_2} + \omega_{\vec{k}_3} - p^0) \right. \\ &\quad \left. + \delta^{(3)}(\vec{k}_1 + \vec{k}_2 + \vec{k}_3 + \vec{p}) \delta^{(1)}(\omega_{\vec{k}_1} + \omega_{\vec{k}_2} + \omega_{\vec{k}_3} + p^0) \right] \\ &\quad \left. \times \left[[f(X, \vec{k}_1) + 1] [f(X, \vec{k}_2) + 1] [f(X, \vec{k}_3) + 1] - f(X, \vec{k}_1) f(X, \vec{k}_2) f(X, \vec{k}_3) \right] \right\} + \mathcal{O}(\lambda^2),\end{aligned}$$

where we stress that the dispersion relations $\omega_{\vec{k}_i}^2[\Phi](X) = \vec{k}_i^2 + M^2[\Phi](X)$ ($i = 1, 2, 3$) contain the background field through the effective mass (3.68).

We explicitly observe a gain-loss structure in the strong-field equation, where the field with unconstrained energy variable p^0 interacts with three particles k_i of strong-field on-shell energies $\omega_{\vec{k}_i}$. The first gain-loss term encodes a $1 - 2$ decay process with the field participating as a dynamical energy reservoir, it can either fuel $k_1 + p \rightarrow k_2 + k_3$ or impede the decay process $k_1 \rightarrow k_1 + k_2 + p$. The second gain-loss contribution acts as a source term where three particles k_i are either produced from the field $p \rightarrow k_1 + k_2 + k_3$ or annihilate into the field $k_1 + k_2 + k_3 \rightarrow p$. Approaching thermal equilibrium, the field becomes constant with the gain-loss structure vanishing due to detailed balance of the thermal distribution functions.

Considering the weak-field regime close to equilibrium, we will discuss an instructive solution of this strong-field equation (3.78) later on as an application in 3.4.6.

We comment here that one can decompose the two-point background field similarly to (3.11) as

$$\Phi(x, y) = \Phi^F(x, y) - \frac{i}{2} \text{sgn}_c(x^0 - y^0) \Phi^\rho(x, y). \quad (3.79)$$

Repeating the above analysis for the RHS, one finds that Φ^ρ drops out entirely, which is what one would expect since $\Phi(x, y)$ is symmetric by construction. This allows us to neglect a distinction between ϕ^+ and ϕ^- in order to later on define an amplitude in the first place, $\phi^+ = \phi^- \equiv \phi$, in particular around (3.100).

Scalar strong-field kinetic equation at leading order in the coupling

With the interactions at LO in the strong-field coupling (3.67) at our disposal, we can proceed to specify the strong-field statistical equation (3.51) and the strong-field kinetic equation (3.57). Their respective drift term on the LHS side does not change under a coupling expansion as the local self energy contributing to the effective mass is fixed by the tadpole, namely (3.68). What does change explicitly is the RHS, where we can now express the self energies to given strong-field coupling order. To this end, we will only specify the collisional functional in the following and refer back to the full statistical or kinetic equation.

In terms of Wightman functions (3.71), the gain-loss structure of the collision functional becomes apparent by employing the following algebraic identity for the RHS expression thereof

$$\Sigma^\rho F - \Sigma^F \rho = -i \left[\Sigma^{-+} G^{+-} - \Sigma^{+-} G^{-+} \right]. \quad (3.80)$$

Going to Wigner space and specifying the explicit form of the self-energies in terms of distribution functions via the KBA (3.32), one can recover an explicit form in terms of collisional integrals. Suppressing the global coordinate dependence by writing $f(X, k) \equiv f_k$ for notational ease, the collision functional at LO in the strong-field coupling reads

$$\begin{aligned} C[f](X, \vec{p}) = & i \frac{\lambda^2}{2} \int_{\mathbb{R}^{12}} \frac{d^4 k_1}{(2\pi)^4} \frac{d^4 k_2}{(2\pi)^4} \frac{d^4 k_3}{(2\pi)^4} \int_0^\infty \frac{dp^0}{2\pi} (2\pi)^4 \delta^{(4)}(k_1 + k_2 + k_3 - p) \\ & \times \rho_{k_2} \rho_{k_3} \rho_p \left[\Phi_{k_1}^{-+} f_{k_2} f_{k_3} [f_p + 1] - \Phi_{k_1}^{+-} [f_{k_2} + 1] [f_{k_3} + 1] f_p \right] \\ & + \mathcal{O}((\partial_p \cdot \partial_X)^1 H) + \mathcal{O}((\partial_p \cdot \partial_X)^2 \Phi). \end{aligned} \quad (3.81)$$

Only the field-dependent contribution $\Sigma^{(2b)}$ enters the collision term, since the field-independent tadpole $\Sigma^{(2a)}$ is dynamically contained in the effective mass (3.68).

We can identify a local scattering amplitude of the form

$$|\mathcal{M}|^2(X, k_1) = \lambda^2 \Phi(X, k_1) \quad (3.82)$$

by pulling out the symmetric background field $\Phi^{+-} = \Phi^{-+} \equiv \Phi$. $|\mathcal{M}|^2$ is isolated solely by defining it as the contribution in the collision functional not contained in the gain-loss term. We will discuss this scattering amplitude and its consequences at length in the following section on particle production in 3.5.

Here we already see that the background field dynamically participates in scattering processes as an energy reservoir, extending the amount of kinematically possible interactions. To recover these, we again map onto positive frequencies by employing the strong-field spectral function (3.49), whereby the collision functional becomes

$$\begin{aligned}
 C[f](X, \vec{p})|_{\rho=\rho(\text{strong})} &\equiv \frac{1}{2} \int_0^\infty \frac{dk_1^0}{2\pi} \int_{\mathbb{R}^9} \frac{d^3k_1}{(2\pi)^3} \frac{d^3k_2}{(2\pi)^3 2\omega_{\vec{k}_2}} \frac{d^3k_3}{(2\pi)^3 2\omega_{\vec{k}_3}} (2\pi)^4 |\mathcal{M}|^2(X, k_1) \\
 &\left\{ \delta^{(3)}(\vec{k}_1 + \vec{k}_2 + \vec{k}_3 - \vec{p}) \delta^{(1)}(k_1^0 + \omega_{\vec{k}_2} + \omega_{\vec{k}_3} - \omega_{\vec{p}}) [f_{\vec{k}_2} f_{\vec{k}_3} [f_{\vec{p}} + 1] - f_{\vec{p}} [f_{\vec{k}_2} + 1] [f_{\vec{k}_3} + 1]] \right. \\
 &+ \delta^{(3)}(\vec{k}_2 + \vec{k}_3 - \vec{k}_1 - \vec{p}) \delta^{(1)}(\omega_{\vec{k}_2} + \omega_{\vec{k}_3} - k_1^0 - \omega_{\vec{p}}) [f_{\vec{k}_2} f_{\vec{k}_3} [f_{\vec{p}} + 1] - f_{\vec{p}} [f_{\vec{k}_2} + 1] [f_{\vec{k}_3} + 1]] \\
 &+ \delta^{(3)}(\vec{k}_1 + \vec{k}_2 - \vec{k}_3 - \vec{p}) \delta^{(1)}(k_1^0 + \omega_{\vec{k}_2} - \omega_{\vec{k}_3} - \omega_{\vec{p}}) [f_{\vec{k}_2} [f_{\vec{k}_3} + 1] [f_{\vec{p}} + 1] - f_{\vec{p}} [f_{\vec{k}_2} + 1] f_{\vec{k}_3}] \\
 &+ \delta^{(3)}(\vec{k}_2 - \vec{k}_1 - \vec{k}_3 - \vec{p}) \delta^{(1)}(\omega_{\vec{k}_2} - k_1^0 - \omega_{\vec{k}_3} - \omega_{\vec{p}}) [f_{\vec{k}_2} [f_{\vec{k}_3} + 1] [f_{\vec{p}} + 1] - f_{\vec{p}} [f_{\vec{k}_2} + 1] f_{\vec{k}_3}] \\
 &+ \delta^{(3)}(\vec{k}_1 + \vec{k}_3 - \vec{k}_2 - \vec{p}) \delta^{(1)}(k_1^0 + \omega_{\vec{k}_3} - \omega_{\vec{k}_2} - \omega_{\vec{p}}) [f_{\vec{k}_2} + 1] f_{\vec{k}_3} [f_{\vec{p}} + 1] - f_{\vec{p}} f_{\vec{k}_2} [f_{\vec{k}_3} + 1] \\
 &+ \delta^{(3)}(\vec{k}_3 - \vec{k}_1 - \vec{k}_2 - \vec{p}) \delta^{(1)}(\omega_{\vec{k}_3} - k_1^0 - \omega_{\vec{k}_2} - \omega_{\vec{p}}) [f_{\vec{k}_2} + 1] f_{\vec{k}_3} [f_{\vec{p}} + 1] - f_{\vec{p}} f_{\vec{k}_2} [f_{\vec{k}_3} + 1] \\
 &+ \delta^{(3)}(\vec{k}_1 + \vec{k}_2 + \vec{k}_3 + \vec{p}) \delta^{(1)}(k_1^0 + \omega_{\vec{k}_2} + \omega_{\vec{k}_3} + \omega_{\vec{p}}) [f_{\vec{k}_2} + 1] [f_{\vec{k}_3} + 1] [f_{\vec{p}} + 1] - f_{\vec{p}} f_{\vec{k}_2} f_{\vec{k}_3}] \\
 &+ \delta^{(3)}(\vec{k}_1 - \vec{k}_2 - \vec{k}_3 - \vec{p}) \delta^{(1)}(k_1^0 - \omega_{\vec{k}_2} - \omega_{\vec{k}_3} - \omega_{\vec{p}}) [f_{\vec{k}_2} + 1] [f_{\vec{k}_3} + 1] [f_{\vec{p}} + 1] - f_{\vec{p}} f_{\vec{k}_2} f_{\vec{k}_3}] \left. \right\} \\
 &+ \mathcal{O}(\lambda^2). \tag{3.83}
 \end{aligned}$$

The processes contained in the collision functional (3.83) describe the possible scattering processes, where the interaction of a particle of momentum p with two particles of momentum k_2 and k_3 is considered, the background field with label k_1 participates in the scattering process as a dynamical energy reservoir. Considering the kinematically forbidden process $p \rightarrow k_2 + k_3$, including the background field facilitates such a decay process to take place by lending energy. In a sense, the processes

$$p + \Phi(k_1) \rightarrow k_2 + k_3, \quad p \rightarrow \Phi(k_1) + k_2 + k_3$$

are equivalent since they describe a $1 \rightarrow 2$ decay process facilitated by drawing energy from the background field.

In the absence of a background field, the dominant contribution to the collision integral is 2-2 scattering [22, 35]. However, 2-2 is suppressed in the strong-field regime at linear order in the strong-field coupling as it scales like $\mathcal{O}(\lambda^2)$. In contrast to conventional zero-field kinetic theory, non-trivial scattering therefore already arises to LO $\mathcal{O}(\lambda)$ in the strong-field regime due to the incorporation of a dynamical background field.

Scalar strong-field kinetic theory at leading order in the coupling

Collecting our results, we present the full strong-field kinetic system employing a leading order expansion in the coupling $\mathcal{O}(\lambda)$ through our strong-field power counting

scheme. This set of equations is equivalently complete to LO in the coupling, LO in propagator gradients and NLO in field-gradients.

Kinetic strong-field equations

$$\left[2p^\mu \frac{\partial}{\partial X^\mu} + \mathcal{F}_\mu[\Phi](X) \frac{\partial}{\partial p_\mu} \right] \Phi(X, p) = -\frac{\lambda^2}{6} \Phi(X, p) \mathcal{G}[\Phi, f](X, p) + \mathcal{O}(\lambda^2) \quad (3.84a)$$

$$\rho(X, p^0, \vec{p}) = -i(2\pi) \operatorname{sgn}(p^0) \delta^{(1)}(p^2 - M^2[\phi](X)) + \mathcal{O}(\lambda^2), \quad (3.84b)$$

$$\begin{aligned} \frac{d}{dt} f(X, \omega_{\vec{p}}, \vec{p}) &= \left[\frac{\partial}{\partial X^0} + v_{i,\text{group}} \frac{\partial}{\partial X_i} + \mathcal{F}_i^{\text{eff}}(X, \omega_{\vec{p}}, \vec{p}) \frac{\partial}{\partial p_i} \right] f(X, \omega_{\vec{p}}, \vec{p}) \\ &= C[f](t, \vec{p})|_{\rho=\rho^{(\text{strong})}} + \mathcal{O}(\lambda^2), \end{aligned} \quad (3.84c)$$

with the effective force defined in (3.56), $\mathcal{G}[\Phi, f](X, p)$ specified in (3.78) and the collision functional $C[f](t, \vec{p})|_{\rho=\rho^{(\text{strong})}}$ explicitly given by (3.83).

These equations facilitate investigations of any observable defined via the Boltzmann-like kinetic equation (3.84c) for strong background fields.

As an application, we will employ this set of strong-field equations in a study of scalar particle production later on in 3.5.

3.4.6 Solution of the weak-field equation to leading order in the coupling

Before we discuss particle production, we want to consider the weak-field regime close to equilibrium to provide for an intuitive understanding of background field dynamics. For the weak-field regime close to equilibrium $F \sim 1$, the coupling counting in the field has to be modified to $\Phi \sim \lambda$.

Therefore, $2-2$ scattering proceeding through the four vertex becomes dominant since $C[f]_{2-2} \sim \mathcal{O}(\lambda^2)$ and scattering processes taking place via the effective three vertex are sub-leading, for example $C[f]_{1-2} \sim \mathcal{O}(\lambda^3)$, since they contain the background field. This exemplifies how the ordering of diagrams is changed going from the weak-field to the strong-field regime. Further, this motivates an adjustment of the gradient-counting relation to

$$(\partial_p \cdot \partial_X) \sim \lambda^2 \quad \Leftarrow \quad (p \cdot \partial_X) f(X, p) = C[f]_{2-2} = \mathcal{O}(\lambda^2). \quad (3.85)$$

Applying the counting rules, the drift term has to be dropped and the free spectral function to be employed. For a spatially homogeneous system, the field equation of motion under the kinetic limit (3.84a) for the weak-field regime at LO $\mathcal{O}(\lambda^2)$ in the coupling becomes

$$\partial_t \ln \Phi(t, p) = \frac{\lambda^2}{12p^0} C[f]_{2-2}(t, p) + \mathcal{O}(\lambda^3), \quad (3.86)$$

with the $2 - 2$ scattering kernel $C[f]_{2-2}$ for example found in [22]. $C[f]_{2-2}$ is independent of the background field since it proceeds through the four vertex. Additionally, since we dropped the drift term, the energies of the scattering participants are on-shell with respect to the free spectral function (3.27). Therefore, the weak-field equation at LO $\mathcal{O}(\lambda^2)$ in the coupling facilitates an exponential solution. This solution then seems to be of infinite order in the coupling. Such a behaviour stems from making a LO coupling approximation on the level of equations of motion, where the solution can then still be of infinite order in the coupling. If one requires to compare with LO coupling expressions, additionally the solution has to be approximated. This solution already selectively incorporates a subset of dynamics which are non-perturbative in the coupling, lending credibility to employing this solution in later studies for weak-field phenomena. In an explicit analysis we have to take the spectral and statistical dynamics into account, as they also scale with the coupling, such that understanding the weak-field dynamics already entails solving the closed strong-field kinetic system (3.84) in the weak-field approximation.

3.5 Particle production in strong-field kinetic theory at leading order in the coupling

In this section we aim to identify mechanisms of particle production based on the derived strong-field kinetic system (3.84). With these equations at our disposal, we will begin by presenting a collisionless $\mathcal{O}(\lambda^0)$ mechanism for particle production which is facilitated by the drift term encoding strong-field fluctuations in the kinetic equation in 3.5.1. Subsequently, we will discuss collisional $\mathcal{O}(\lambda)$ particle production as facilitated by inelastic scattering processes weighted with a dynamical scattering amplitude. Towards quantifying and understanding this mechanism, the concept of scattering amplitudes in nonequilibrium kinetic theory and mechanisms of reduction towards scattering amplitudes in vacuum theory is investigated in 3.5.2. The explicit mechanism through inelastic processes is then elaborated on, where a comparison of $1 \rightarrow 2$ decay rates in NeqQFT and vQFT in 3.5.3 will present itself as a further connection between nonequilibrium dynamics and the vacuum formulation of particle production in the language of scattering amplitudes and decay rates. Finally, by a comparison we conclude that the full strong-field kinetic system with a focus on the strong-field equation (3.84a) generalizes the standard framework for the kinetic description of near-equilibrium Bose-Einstein condensation.

3.5.1 Collisionless particle production in strong-field kinetic theory

Inelastic scattering processes encoded in the collision integral $C[f]$ can change the particle number of the system, they are however sub-leading to the drift term in a strong-field coupling expansion¹¹. The drift term encodes a collisionless $\mathcal{O}(\lambda^0)$ change in particle number facilitated by fluctuations of the background field. To recover dominant particle production effects, it will therefore suffice to ignore collisions $C \equiv 0$ in the following analysis for leading-order particle production in kinetic theory. Even in the absence of collisions, a collisionless damping of the field oscillations towards a minimum configuration is present from the particles interacting with each other only through the background field, as encoded in the feedback effect through the drift term.

Therefore, the Boltzmann-like strong-field kinetic equation (3.84c) reduces to

$$\frac{\partial}{\partial X^0} f(X, \omega_{\vec{p}}, \vec{p}) = - \left[v_{i,\text{group}} \frac{\partial}{\partial X_i} + \mathcal{F}_i^{\text{eff}}(X, \omega_{\vec{p}}, \vec{p}) \frac{\partial}{\partial p_i} \right] f(X, \omega_{\vec{p}}, \vec{p}). \quad (3.87)$$

This kinetic equation can be rephrased into an equation for the total particle number. To this end, we can define a particle number density and a total particle number

$$n(X) = \int \frac{d^3 p}{(2\pi)^3} f(X, \vec{p}), \quad N(X^0) = \int d^3 X n(X). \quad (3.88)$$

¹¹In the strong-field regime, the collision kernel contains processes at LO in the coupling $\mathcal{O}(\lambda^2 \Phi) = \mathcal{O}(\lambda)$, whereas the drift term contains a contribution which is $\mathcal{O}(\lambda \Phi) = \mathcal{O}(\lambda^0)$ in a coupling expansion.

Following a procedure formulated for asymptotic pair production in QED [29], we will now integrate this equation over \vec{p} and t to recover a change in total particle number facilitated by the drift term

$$\begin{aligned} N(t) - N(-\infty) &= \int \frac{d^3p}{(2\pi)^3} \int_{-\infty}^t dX^0 \int d^3X \frac{\partial}{\partial X^0} f(X^0, \vec{p}) \\ &= - \int \frac{d^3p}{(2\pi)^3} \int_{-\infty}^t dX^0 \int d^3X \left[v_{i,\text{group}} \frac{\partial}{\partial X_i} + \mathcal{F}_i^{\text{eff}}(X, \omega_{\vec{p}}, \vec{p}) \frac{\partial}{\partial p_i} \right] f(X, \omega_{\vec{p}}, \vec{p}). \end{aligned} \quad (3.89)$$

Specifying to a spatially homogeneous system, spatial gradients in the kinetic equation vanish

$$\partial_t f(t, \vec{p}) \approx -\mathcal{F}_i^{\text{eff}}(t, \vec{p}) \frac{\partial}{\partial p_i} f(t, \vec{p}) = -\frac{\partial M^2(t)}{\partial t} \frac{1}{2p^i} \frac{\partial}{\partial p_i} f(t, \vec{p}), \quad (3.90)$$

such that we explicitly find

$$\begin{aligned} N(t) - N(-\infty) &= \int \frac{d^3p}{(2\pi)^3} \int_{-\infty}^t dt' \partial_{t'} f(t', \vec{p}) \\ &= - \int_{-\infty}^t dt' \frac{\partial M^2(t')}{\partial t'} \int \frac{d^3p}{(2\pi)^3} \frac{1}{2p^i} \frac{\partial}{\partial p_i} f(t', \vec{p}) \\ &= -\frac{1}{2} \int_{-\infty}^t dt' \frac{\partial M^2(t')}{\partial t'} \int \frac{d^3p}{(2\pi)^3} \left[\frac{1}{p_x^2} + \frac{1}{p_y^2} + \frac{1}{p_z^2} \right] f(t', \vec{p}). \end{aligned} \quad (3.91)$$

Particle production at time t will then be encoded by $N(t) - N(-\infty) > 0$, where one can recover asymptotic expressions for $t \rightarrow \infty$.

For the strong-field regime $\phi \sim \mathcal{O}(\lambda^{-\frac{1}{2}})$ in a two-loop expansion of Γ_2 , the tadpole contribution in the effective mass (3.68) is sub-leading in a coupling counting such that one can employ

$$\partial_t M^2(t) = \frac{\lambda}{2} \left[\frac{2}{3} \phi(t) \partial_t \phi(t) + \partial_t F(t, t) \right] = \frac{\lambda}{3} \phi(t) \partial_t \phi(t) + \mathcal{O}(\lambda) \quad (3.92)$$

for this $\mathcal{O}(\lambda^0)$ process. The resulting particle number can be obtained from (3.91), where suitable initial conditions

$$f_0(\vec{p}) := f(t = -\infty, \vec{p}), \quad \phi_0 := \phi(t = -\infty) \quad (3.93)$$

have to be specified in conjunction with a solution of the background field dynamics (3.84a). A non-kinetic analysis of the drift term is necessary if one is interested in the early-time and small scale behaviour of this mechanism of particle production in the form of dephasing and dissipation, where a treatment facilitated by a mean-field approximation can be found in [24]

Collisionless particle production of gap-less modes

In this section we want to discuss another collisionless mechanism of particle production in the presence of a tachyonic instability which is absent in conventional kinetic

descriptions.

Referring back to the discussion in (3.50), gap-less modes are not consistent with the spectral equation (3.48) if one employs the strong-field spectral function (3.49). We consider again the support of the delta functions

$$\left[p^\mu \frac{\partial}{\partial X^\mu} + \mathcal{F}_\mu \frac{\partial}{\partial p_\mu} \right] \rho^{(\text{strong})}(X, p) \sim \frac{\delta^{(1)}(p^0 - \omega_{\vec{p}}) \delta^{(1)}(p^0)}{p^0}, \quad (3.94)$$

which is non-vanishing if the field-dependent dispersion relation vanishes

$$p^0 = 0 \quad \text{and} \quad p^0 = \pm \sqrt{\vec{p}^2 + m^2 + \frac{\lambda}{2} \left[\frac{1}{3} \phi^2(X) + F(X, X) \right]}. \quad (3.95)$$

For the considered real scalar field with $\lambda > 0$, we have $\phi^2(X) > 0$ and the equal-time tadpole contribution $F(X, X) > 0$ has to be positive since it describes the variance of the fields. The dispersion relation can then only vanish for a negative mass

$$0 \stackrel{!}{=} p^0 = \pm \sqrt{\vec{p}^2 + M^2(X)} \quad \Leftrightarrow \quad -m^2 = \vec{p}^2 + \frac{\lambda}{2} \left[\frac{1}{3} \phi^2(X) + F(X, X) \right]. \quad (3.96)$$

Then, the strong-field spectral equation of motion (3.48) is not solved by the strong-field spectral function (3.49) but exhibits an additional term

$$\left[p^\mu \frac{\partial}{\partial X^\mu} + \mathcal{F}_\mu \frac{\partial}{\partial p_\mu} \right] \rho^{(\text{strong})}(X, p) = -i2\pi \frac{\partial M^2(X)}{\partial X^0} \frac{\delta^{(1)}(\omega_{\vec{p}})}{\omega_{\vec{p}}}. \quad (3.97)$$

Such a behaviour is reminiscent of a tachyonic instability. Instabilities are early-time phenomena conventionally absent in a late-time kinetic description. Parametric instabilities do not appear as oscillations are averaged out by the gradient expansion and tachyonic instabilities conventionally are not present since the triggering tachyonic mass $m^2 < 0$ drops out upon considering differences of the 2PI equations of motion for the kinetic description. However, the tachyonic instability is still present in our kinetic description since the employed strong-field spectral function (3.49) is not the solution of the strong-field spectral equation (3.48), but rather the solution of the non-subtracted 2PI spectral equation (3.25) in Wigner space with

$$(p^2 - M^2) \rho(X, p) = 0 \quad \Rightarrow \quad \rho \sim \delta^{(1)}(p^2 - M^2). \quad (3.98)$$

This discussed inconsistency (3.50) therefore facilitates such an instability to be present in our strong-field kinetic description. Furthermore, investigating tachyonic instabilities in kinetic theory requires one to consider a dynamical background field since the instability drops out for a constant field due to the derivative $\partial_X M^2$.

This instability can then serve as a mechanism for collisionless particle production through the drift term. As was eluded to in footnote 8, this mechanism becomes apparent by considering the explicit derivation of the strong-field kinetic equation (3.57) from the strong-field statistical equation (3.51). The drift term will then encode the pro-

duction of gap-less modes. Schematically for a spatially homogeneous system, we can uncover such a mechanism by being specific about when we go on-shell with respect to the strong-field spectral function (3.49) in the course of this derivation

$$\begin{aligned} \int_0^\infty dp^0 \frac{\partial M^2}{\partial t} \frac{\partial}{\partial p_0} F(t, p) &\sim \int_0^\infty dp^0 \frac{\partial M^2}{\partial t} \frac{\partial}{\partial p_0} (\rho(t, p) f(t, p)) \\ &\sim -\frac{\partial M^2}{\partial t} \int_{\mathbb{R}} dp^0 \delta^{(1)}(p^0) \rho(t, p) f(t, p), \end{aligned}$$

where the last step follows since the distribution function vanishes for $p^0 \rightarrow \infty$. With the spectral function remaining unspecified, the second step becomes possible and we observe that the zero-mode is singled out. If we now go on-shell by employing the strong-field spectral function (3.49), then we recover a mechanism of particle production from the drift term

$$\begin{aligned} \frac{\partial M^2(t)}{\partial t} \frac{\partial}{\partial p_0} F(X, p) &\rightarrow \frac{\partial M^2(t)}{\partial t} \int_{\mathbb{R}} dp^0 \delta^{(1)}(p^0) \frac{\delta(p^0 - \omega_{\vec{p}})}{2p^0} f(t, p) \\ &\sim \frac{\partial M^2(t)}{\partial t} \frac{\delta^{(1)}(\omega_{\vec{p}})}{\omega_{\vec{p}}} f(t, \omega_{\vec{p}}, \vec{p}). \end{aligned} \quad (3.99)$$

This particle production takes place in the momentum shell defined by the condition $|\vec{p}|^2 = -M^2$. With our above discussion around (3.97) in mind, this particle growth could be connected to the presence of a tachyonic instability.

In contrast, if we go on-shell with respect to the strong-field spectral function early on in the derivation, then this mechanism is absent and we recover collisionless particle production as driven by the background field (3.91).

Neglecting the drift term in the kinetic derivation and therefore resorting to the free spectral function (3.27), the tachyonic instability and this mechanism for particle production of gap-less modes (3.99) will not be present and is therefore a distinct feature of the strong-field kinetic system (3.84).

3.5.2 Scattering amplitudes in strong-field kinetic theory

In this and in the following sections we want to present collisional particle production as facilitated by inelastic scattering processes. The collisions appear sub-leading in a coupling counting and will make effects of dephasing and dissipation towards a minimum configuration of the field even more pronounced [24]. To this end, the meaning of scattering theory in a nonequilibrium setting has to be discussed. Collectively, these sections will provide us with a more intuitive understanding of how particle production mitigated through scattering amplitudes such as Higgspllosion could arise in nonequilibrium theory. In a first step, we will therefore aim to make an identification between tree-level scattering expressions from vacuum and from nonequilibrium theory. This is far away from identifying the Higgspllosion rate (2.1) in the nonequilibrium formalism, but it will provide the foundation for further investigation.

We have identified a squared amplitude in the collision functional (3.81) of the kinetic

equation (3.84c), which is

$$|\mathcal{M}|^2(X) = \int_{\mathbb{R}^4} \frac{d^4k}{(2\pi)^4} |\mathcal{M}|^2(X, k) = \lambda^2 \int_{\mathbb{R}^4} \frac{d^4k}{(2\pi)^4} \Phi(X, k), \quad (3.100)$$

where we included the integration for comparison purposes with the vacuum case. From the perspective of kinetic theory, scattering amplitudes quantify the probability for a change in occupation number for a given interaction in real-time dynamics. This amplitude (3.100) applies to all the different kinematical scattering events contributing at LO in the coupling for the strong-field regime. We can not distinguish between different channels solely from the Boltzmann-like kinetic equation (3.84c). Considering the squared amplitude in the context of one of eight accompanying delta-functions over energies in (3.83), we can however explicitly talk about physically distinct processes. At leading order in the coupling, the amputated scattering amplitude in vQFT was given in 2.4 within (2.12) and explicitly reads

$$|\mathcal{M}|_{\text{vac}}^2 = \lambda^2 v^2. \quad (3.101)$$

Comparing with (3.100), we observe that if the system has equilibrated to the value v , translation invariance is restored and there is no more energy exchange and the expressions agree

$$\Phi(X, p) \xrightarrow{t \rightarrow \infty} v^2. \quad (3.102)$$

We can make the observation that the thermalized VEV is obtained explicitly by setting the momentum label of the background field to zero, that is we make the ansatz

$$\Phi(X, p) \stackrel{\text{vQFT} \leftrightarrow \text{NeqQFT}}{=} (2\pi)^4 v^2 \delta^{(3)}(\vec{p}) \delta^{(1)}(p^0), \quad (3.103)$$

where the time-independence can either be obtained by simply assuming a constant background field or by considering expressions in the asymptotic future. The prefactor is included for normalization purposes. Note that such an assignment is artificially put in by hand for conventional calculations involving a background field, thereby effectively neglecting its dynamics and treating it as a constant external field [36].

This identification (3.103) is one of the main achievements of this thesis, in that we have found an intersection between nonequilibrium and vacuum theory by a prescription of how to reduce the additional complexity. Only upon considering the complete dynamics of the system can one self-consistently understand how the background field thermalizes and becomes the VEV. We will discuss the emergent scattering picture in kinetic theory in the following.

With the complete set of kinetic equations at our disposal (3.84), one can proceed to analyze the dynamics of the scattering amplitude (3.100). Depending on the fluctuations of the background field, the scattering amplitude could grow substantially, indicating particle production.

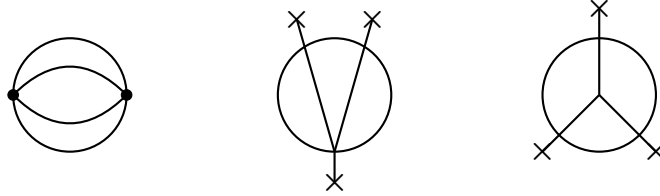
Scattering amplitudes in a nonequilibrium setting

As expected, the more general NeqQFT framework contains conventional vQFT as a special case such that vQFT results can be reproduced self-consistently. The above comparison involves subtleties as global amplitudes can not simply be defined in a dynamical nonequilibrium treatment since the nonequilibrium amplitude (3.100) is inherently local, $|\mathcal{M}|^2 = |\mathcal{M}|^2(X)$. Obtaining a global amplitude necessitates a self-consistent description encompassing the dynamics of the background field and of the distribution function. The local probability of a scattering event changes with the distribution function being a local object. In comparison to vQFT, total scattering probabilities can not be defined in NeqQFT due to the dynamical build up of distribution functions in the process of thermalization. Global scattering amplitudes can be solved for if the complete knowledge of the dynamics is known throughout time evolution.

Crucially, the local amplitude (3.100) is quadratically dependent on the background field, whose dynamical evolution is described by its respective equation of motion.

Amplitudes at NLO in the coupling

To this end, we want to discuss the translation procedure further by considering the amplitudes which one could parametrically isolate at NLO in the strong-field coupling. Diagrammatically, the contributing 2PI diagrams are



We emphasize again that we are counting couplings in the strong-field regime, which is why λ^3 and λ^4 terms will appear at $\mathcal{O}(\lambda^2)$.

The resulting strong-field kinetic equation will contain contributions from the different diagrams, it is therefore not straightforward to isolate one global expression for the scattering amplitude. However, we schematically indicate a scattering amplitude which is NLO in the strong-field coupling with the form of the Boltzmann-like kinetic equation for a spatially homogeneous system, neglecting numerical factors and introducing an implicit integral notation of Wigner momenta $\int_p \equiv \frac{d^4 p}{(2\pi)^4}$

$$\partial_t f(t, \vec{p}) \sim \int dp^0 \int_{k_1 \dots k_n \dots k_m} (2\pi)^4 \delta^{(4)}(p - k_1 - \dots - k_m) |\mathcal{M}|^2(\{t_i\}, \{k_j | j \neq 1 \dots n\}) \\ \rho_{k_1} \dots \rho_{k_n} \times \text{GL}[f_1, \dots, f_n, f_p],$$

where GL contains the gain-loss structure consisting of distribution functions f and their respective Bose-enhanced form $[f + 1]$ in combinations which are dictated by the kinematic process at hand. Keeping in mind that this identification still requires integration

over a multitude of labels, we find

$$|\mathcal{M}|_{\mathcal{O}(\lambda^2)}^2(t, t', t'') \sim C_1 \times \lambda^2 \quad (3.104)$$

$$+ C_2 \times \lambda^3 \int_k [C_3 \times \Phi(k, t) + C_4 \times \Phi(k, t')] + C_5 \times \lambda^4 \int_{k,q} \Phi(k, t) \Phi(q, t'').$$

At increasing loop order, we will therefore have to consider a growing number of diagrams made up of combinations of the four and effective three vertex. Although describing a non-equilibrium framework, we are still treating scalar field theory whose diagrams do not interfere destructively, which is exactly what initially lead to the factorial or exponential growth of amplitudes for multi-particle processes 2.1. Therefore, the resulting amplitude will contain ever more terms at higher powers in the coupling, where every diagram involving the three vertex involves powers of the background field.

Summarizing, we can observe that the identification of scattering expressions becomes increasingly more involved and non-trivial at higher loop orders. It is not at all clear whether these scattering amplitudes will resum to a n -point amplitude or rate which grows exponentially like for the original Higgsplosion rate (2.1).

3.5.3 Collisional particle production through decay rates in strong-field kinetic theory

In order to make progress towards a comparison with scattering processes at leading order in the coupling as described for vQFT in 2.4.1, we will consider the strong-field kinetic equation (3.84c) for small occupations $f \ll 1$, therefore close to vacuum.

The subsequent scheme to identifying a rate is taken from [19], where other definitions are equally possible [37].

Small occupations in the strong-field regime

Since we are considering a linearised treatment around vacuum, we will linearise the on-shell distribution functions $f \ll 1$. This will result in a reduction of leading order decay rates. For such settings close to vacuum, one may drop $2 \rightarrow 1$ and $3 \rightarrow 0$ processes entirely, since they contain no linear terms and are therefore suppressed¹². Note that $2 - 2$ processes automatically drop out by symmetry of the distribution function under the integral. This is what we would expect since $2 - 2$ elastic scatterings are particle number conserving. The remaining scattering processes involving the field ϕ change the particle number.

The strong-field Boltzmann-like kinetic equation (3.84c) can again be cast into an equation for the total particle number, which will be instructive to understand particle production. To this end, we will neglect collisionless $\mathcal{O}(\lambda^0)$ particle production as facilitated by the drift term which we already discussed in 3.5.1, and only consider collisional $\mathcal{O}(\lambda)$ particle production for now. Furthermore, we will specialize to a spatially homogeneous

¹²As was commented on in [29], this suppression by distribution functions is analogous to the conventional argument of phase space suppression.

system for comparison reasons. We are aiming here to identify and compare expressions for the $1 \rightarrow 2$ decay rate driving particle production at LO in the coupling. This will provide us with an intuition for the $1^* \rightarrow n$ decay rates which we are interested in for Higgspllosion. Following the procedure in [19], we bring the strong-field statistical kinetic equation into an exponential form, explicitly

$$\partial_t N(t)|_{f \ll 1} = \int \frac{d^3 p}{(2\pi)^3} \Gamma(t, \vec{p}) f(t, \vec{p}) + N_{\text{source}}(t) + \mathcal{O}(f^2), \quad (3.105)$$

which will enable us to identify a decay rate for the different processes. Again, particle production will then be encoded by $\partial_t N(t) > 0$.

Suitably approximating for small occupations, relabelling momenta under the integrals and employing the strong-field spectral function, we find

$$\begin{aligned} \partial_t N(t)|_{f \ll 1} = & \frac{1}{2} \int_{\mathbb{R}^{12}} \frac{d^3 p}{(2\pi)^3 2\omega_{\vec{p}}} \frac{d^3 k_1}{(2\pi)^3} \frac{d^3 k_2}{(2\pi)^3 2\omega_{\vec{k}_2}} \frac{d^3 k_3}{(2\pi)^3 2\omega_{\vec{k}_3}} \int_0^\infty \frac{dk_1^0}{2\pi} (2\pi)^4 |\mathcal{M}|^2(t, k) \\ & \left[\delta^{(3)}(\vec{k}_1 + \vec{k}_2 + \vec{k}_3 - \vec{p}) \delta^{(1)}(k_1^0 + \omega_{\vec{k}_2} + \omega_{\vec{k}_3} - \omega_{\vec{p}}) \right. \\ & \left. + \delta^{(3)}(\vec{k}_2 + \vec{k}_3 - \vec{k}_1 - \vec{p}) \delta^{(1)}(\omega_{\vec{k}_2} + \omega_{\vec{k}_3} - k_1^0 - \omega_{\vec{p}}) \right] f(t, \vec{p}) \\ & + N_{\text{source}}(t), \end{aligned} \quad (3.106)$$

where the source term encodes particle production from the vacuum driven by the field

$$\begin{aligned} N_{\text{source}}(t) = & \frac{1}{2} \int_{\mathbb{R}^{12}} \frac{d^3 p}{(2\pi)^3 2\omega_{\vec{p}}} \frac{d^3 k_1}{(2\pi)^3} \frac{d^3 k_2}{(2\pi)^3 2\omega_{\vec{k}_2}} \frac{d^3 k_3}{(2\pi)^3 2\omega_{\vec{k}_3}} \int_0^\infty \frac{dk_1^0}{2\pi} (2\pi)^4 |\mathcal{M}|^2(t, k) \\ & \times \left[\delta^{(3)}(\vec{k}_1 + \vec{k}_2 + \vec{k}_3 + \vec{p}) \delta^{(1)}(k_1^0 + \omega_{\vec{k}_2} + \omega_{\vec{k}_3} + \omega_{\vec{p}}) \right. \\ & \left. + \delta^{(3)}(\vec{k}_1 - \vec{k}_2 - \vec{k}_3 - \vec{p}) \delta^{(1)}(k_1^0 - \omega_{\vec{k}_2} - \omega_{\vec{k}_3} - \omega_{\vec{p}}) \right]. \end{aligned} \quad (3.107)$$

These processes are not proportional to a distribution function since they correspond to $0 \rightarrow 3$ processes, which do not require particles to take place. In contrast, a $1 \rightarrow 2$ scattering is the more probable the more particles are present, therefore the larger f is, which is why they scale with f . Again, the two processes contained in $N_{\text{source}}(t)$ describe production of particles from the vacuum, respectively $\Phi(k_1) \rightarrow p + k_2 + k_3$, and $0 \rightarrow \Phi(k_1) + p + k_2 + k_3$, which are formally the same process $0 \rightarrow 3$ facilitated by drawing from the background field as a dynamical energy reservoir. These processes (3.107) are responsible for the phenomenon of vacuum decay, where the instability of the vacuum has to be interpreted in the context of the vacuum being a dynamical object. We can then identify the rate at leading order in the coupling to be

$$\begin{aligned} \Gamma^{(2b)}(t, \vec{p}) = & \frac{1}{2} \frac{1}{2\omega_{\vec{p}}} \int_{\mathbb{R}^{12}} \frac{d^3 k_1}{(2\pi)^3} \frac{d^3 k_2}{(2\pi)^3 2\omega_{\vec{k}_2}} \frac{d^3 k_3}{(2\pi)^3 2\omega_{\vec{k}_3}} \int_0^\infty \frac{dk_1^0}{2\pi} (2\pi)^4 |\mathcal{M}|^2(t, k) \\ & \left[\delta^{(3)}(\vec{k}_1 + \vec{k}_2 + \vec{k}_3 - \vec{p}) \delta^{(1)}(k_1^0 + \omega_{\vec{k}_2} + \omega_{\vec{k}_3} - \omega_{\vec{p}}) \right. \\ & \left. + \delta^{(3)}(\vec{k}_2 + \vec{k}_3 - \vec{k}_1 - \vec{p}) \delta^{(1)}(\omega_{\vec{k}_2} + \omega_{\vec{k}_3} - k_1^0 - \omega_{\vec{p}}) \right] \end{aligned} \quad (3.108)$$

This nonequilibrium rate contains two processes which differ by the field contributing to the decaying particle or by energy being stored in the field after the particle decayed. Both processes transport energy between particles and the field. They describe decay process $p \rightarrow k_2 + k_3$, which is distinguished by whether the background field fuels the decay $p + k_1 \rightarrow k_2 + k_3$ or whether the decay transports energy into the field $p \rightarrow k_1 + k_2 + k_3$. As we commented on earlier, they are technically equivalent since the $p \rightarrow k_2 + k_3$ process is facilitated by drawing energy from the dynamical background field.

Comparison with vacuum decay rate

Having identified a decay rate, we can compare its contents to the decay rates found for conventional ϕ^4 theory in vQFT. The background field assumes a thermalized constant value in vacuum theory such that the tree-level decay process $1 \rightarrow 2$ is kinematically forbidden. Isolating the corresponding decay rate (2.12) for comparison purposes only we have explicitly

$$\Gamma_{p \rightarrow k_2 + k_3}^{\text{vac}}(\vec{p}) = \frac{1}{2} \frac{1}{2\omega_{\vec{p}}} \int \frac{d^3k_2}{(2\pi)^3 2\omega_{\vec{k}_2}} \frac{d^3k_3}{(2\pi)^3 2\omega_{\vec{k}_3}} (2\pi)^4 \delta^{(4)}(p - k_2 - k_3) \lambda^2 v^2, \quad (3.109)$$

We stress that the particles p, k_2 , and k_3 are on-shell with respect to the renormalized vacuum mass-shell $p^2 = m_{\text{R,vac}}^2$. The decay rate which was identified at LO in the strong-field coupling from kinetic theory (3.108) contains the equivalent processes $p + k_1 \rightarrow k_2 + k_3$ and $p \rightarrow k_1 + k_2 + k_3$, of which we isolate the former

$$\Gamma_{p \rightarrow k_2 + k_3}^{(2b)}(t, \vec{p}) = \frac{1}{2} \frac{1}{2\omega_{\vec{p}}} \int_{\mathbb{R}^{12}} \frac{d^3k_1}{(2\pi)^3} \frac{d^3k_2}{(2\pi)^3 2\omega_{\vec{k}_2}} \frac{d^3k_3}{(2\pi)^3 2\omega_{\vec{k}_3}} \int_0^\infty \frac{dk_1^0}{2\pi} (2\pi)^4 |\mathcal{M}|^2(t, k) \delta^{(3)}(\vec{k}_1 + \vec{k}_2 + \vec{k}_3 - \vec{p}) \delta^{(1)}(k_1^0 + \omega_{\vec{k}_2} + \omega_{\vec{k}_3} - \omega_{\vec{p}}) \quad (3.110)$$

In contrast, this describes decay processes which are on-shell with respect to the effective field-dependent mass-shell $p^2 = M^2[\phi](t)$.

Comparing (3.109) and (3.110), we observe a qualitative difference. The kinetic decay rate is time-dependent, which stems from the dynamical contribution of the background field itself. This has to be absent in the thermal expression since the background field becomes constant in thermal equilibrium.

We can explicitly identify one with the other by virtue of the established reduction procedure to go from the background field to the VEV, namely (3.103). This brings us to

$$\begin{aligned} & v^2 \delta^{(1)} \left(\sqrt{\vec{k}_2^2 + m_{\text{R,vac}}^2} + \sqrt{\vec{k}_3^2 + m_{\text{R,vac}}^2} - \sqrt{\vec{p}^2 + m_{\text{R,vac}}^2} \right) \delta^{(3)}(\vec{k}_2 + \vec{k}_3 - \vec{p}) \stackrel{\text{vQFT} \leftrightarrow \text{NeqQFT}}{=} \\ & \int \frac{d^4k_1}{(2\pi)^4} \Phi(t, k_1) \left[\delta^{(3)}(\vec{k}_1 + \vec{k}_2 + \vec{k}_3 - \vec{p}) \delta^{(1)}(k_1^0 + \omega_{\vec{k}_2} + \omega_{\vec{k}_3} - \omega_{\vec{p}}) \right]_{\omega_{\vec{p}} := \sqrt{\vec{p}^2 + M^2(t)}} \\ & \stackrel{(3.103)}{=} v^2 \delta^{(1)} \left(\sqrt{\vec{k}_2^2 + M^2(t)} + \sqrt{\vec{k}_3^2 + M^2(t)} - \sqrt{\vec{p}^2 + M^2(t)} \right) \delta^{(3)}(\vec{k}_2 + \vec{k}_3 - \vec{p}). \quad (3.111) \end{aligned}$$

In our identification (3.111) we are considering energies on the LHS which are on-shell with respect to the vacuum renormalized mass $p^2 = m_{\text{R,vac}}^2$ since they are defined as eigenstates to the translation operator P^μ ¹³. Both expressions agree upon making the identification that the late-time effective mass corresponds to the renormalized mass in vacuum theory, such that

$$t > t_{\text{therm.}} \quad \Rightarrow \quad m_{\text{R,vac}}^2 \stackrel{!}{=} M^2. \quad (3.112)$$

Such an identification is an intersection towards understanding mass renormalization in vacuum and in a nonequilibrium setting. The thermalized physical mass is associated with the dynamical mass shift generated through incorporating the interactions of the system resulting from the time evolution of the spectral function from initialization all the way through to thermalization.

Therefore, we can recover vacuum results to remarkable agreement within this framework, where the corresponding nonequilibrium expressions prior to the reduction scheme (3.103) contain more information on the dynamics of the system.

3.5.4 Towards Bose-Einstein condensation

Specializing the strong-field equation (3.84a) to a spatially homogeneous system

$$2p^0 \partial_t \Phi(t, p) = \frac{\lambda^2}{6} \Phi(t, p) \int_{\mathbb{R}^9} \frac{d^3 k_1 d^3 k_2 d^3 k_3}{(2\pi)^9 2\omega_{\vec{k}_1} [\Phi](X) 2\omega_{\vec{k}_2} [\Phi](X) 2\omega_{\vec{k}_3} [\Phi](X)} (2\pi)^4 \quad (3.113)$$

$$\left\{ 3 \left[\delta^{(3)}(\vec{k}_2 + \vec{k}_3 - \vec{k}_1 - \vec{p}) \delta^{(0)}(\omega_{\vec{k}_2} + \omega_{\vec{k}_3} - \omega_{\vec{k}_1} - p^0) \right. \right.$$

$$\left. + \delta^{(3)}(\vec{k}_2 + \vec{k}_3 + \vec{p} - \vec{k}_1) \delta^{(0)}(\omega_{\vec{k}_2} + \omega_{\vec{k}_3} + p^0 - \omega_{\vec{k}_1}) \right]$$

$$\times \left[[f(X, \vec{k}_1) + 1] f(X, \vec{k}_2) f(X, \vec{k}_3) - f(X, \vec{k}_1) [f(X, \vec{k}_2) + 1] [f(X, \vec{k}_3) + 1] \right]$$

$$+ \left[\delta^{(3)}(\vec{k}_1 + \vec{k}_2 + \vec{k}_3 - \vec{p}) \delta^{(1)}(\omega_{\vec{k}_1} + \omega_{\vec{k}_2} + \omega_{\vec{k}_3} - p^0) \right.$$

$$\left. + \delta^{(3)}(\vec{k}_1 + \vec{k}_2 + \vec{k}_3 + \vec{p}) \delta^{(1)}(\omega_{\vec{k}_1} + \omega_{\vec{k}_2} + \omega_{\vec{k}_3} + p^0) \right]$$

$$\times \left[[f(X, \vec{k}_1) + 1] [f(X, \vec{k}_1) + 1] [f(X, \vec{k}_3) + 1] - f(X, \vec{k}_1) f(X, \vec{k}_2) f(X, \vec{k}_3) \right] \Big\},$$

we observe that the strong-field equation (3.84a) generalizes the standard description of near-equilibrium Bose-Einstein condensation through zero-field kinetic theory by Semikoz and Tkachev [38]. This is shown by an explicit comparison in the following. They make an ad-hoc ansatz for the on-shell distribution function as (equation (2.8 – 2.9b) therein)

$$\tilde{f} = f(\omega_{\vec{p}}, t) + (2\pi)^3 n_c(t) \delta^{(3)}(\vec{p}), \quad (3.114)$$

where the second term describes the condensate. From their non-relativistic kinetic equation (equation (2.1) therein) for classical wave kinetics they obtain an equation for

¹³Explicitly, $p^0 = H$ implies on-shell eigenvalues $E_p = \hbar \omega_p$ with $\omega_{\vec{p}}$ being the free dispersion relation $\omega_{\vec{p}}^2 = \vec{p}^2 + m_{\text{R,vac}}^2$

the gas $f(\omega_{\vec{p}}, t)$ and one for the condensate $n_c(t)$, where in particular the latter is given for our notation by

$$\partial_t n_c(t) = \frac{\lambda^2 n_c(t)}{64\pi^3 m} \int_0^\infty d\omega_{\vec{k}_2} d\omega_{\vec{k}_3} \left[f_{\vec{k}_2} f_{\vec{k}_3} - f_{\vec{k}_1} [1 + f_{\vec{k}_2} + f_{\vec{k}_3}] \right]_{\omega_{\vec{k}_1} = \omega_{\vec{k}_2} + \omega_{\vec{k}_3}}. \quad (3.115)$$

Isolating the non-source term in the strong-field equation of motion and multiplying out the Bose-enhanced gain-loss structure, we obtain a similar expression for the relativistic case

$$\begin{aligned} \partial_t \Phi(t, p) \cong & \frac{\lambda^2 \Phi(t, p)}{64\pi^3 p^0} \int \frac{d^3 k_2 d^3 k_3}{(2\pi)^2 2\omega_{\vec{k}_2} 2\omega_{\vec{k}_3}} \left[f_{\vec{k}_2} f_{\vec{k}_3} - f_{\vec{k}_1} [f_{\vec{k}_2} + f_{\vec{k}_3} + 1] \right] \\ & \left[\delta^{(3)}(\vec{k}_2 + \vec{k}_3 - \vec{k}_1 - \vec{p}) \delta^{(0)}(\omega_{\vec{k}_2} + \omega_{\vec{k}_3} - \omega_{\vec{k}_1} - p^0) \right. \\ & \left. + \delta^{(3)}(\vec{k}_2 + \vec{k}_3 + \vec{p} - \vec{k}_1) \delta^{(0)}(\omega_{\vec{k}_2} + \omega_{\vec{k}_3} + p^0 - \omega_{\vec{k}_1}) \right]. \end{aligned} \quad (3.116)$$

Comparing (3.115) and (3.116), we observe that the field equation describes the off-shell scattering into and out of the condensate, which is facilitated by the unconstrained energy p^0 variable of the condensate. Such a distinction is not possible in the on-shell framework of (3.115). Furthermore, the strong-field equation (3.113) is able to describe off-shell annihilation into and production out of the condensate via the source-term. Overall, the description of condensation facilitated by an overoccupation of the zero mode is described through the complete and closed strong-field kinetic system (3.84), where one can consider condensate dynamics by the field and statistical dynamics independently. The field equation therefore generalizes the framework by Semikoz and Tkachev [38].

Condensation is a scattering phenomenon, which is why we were able to neglect the drift term in the strong-field equation (3.84a) for this comparison. Furthermore, the regime of condensation is one of low temperature and large occupations, where the occupations can however not exceed

$$\rho < F < 1/\lambda \quad (3.117)$$

to guarantee the validity of the loop expansion.

We conclude that Bose-Einstein condensation is therefore well-described within our framework, where $\Phi = \phi^2$ serves as an order parameter for condensation instead of the ad-hoc condensate mode $n_c(t)$. To investigate such a near-equilibrium Bose-Einstein condensate, for example in the context of Higgspllosion, an explicit understanding of the initial conditions and a subsequent solution of the complete strong-field kinetic system (3.84) has to be provided.

3.6 Conclusion

In this work, we have attempted to provide the foundation for studying strong-field particle production processes in a nonequilibrium setting, where we derived the necessary framework in the form of a strong-field kinetic system. By isolating mechanisms for particle production such as collisionless production of modes through a drift term encoding strong-field fluctuations, collisional inelastic scatterings and making contact with near-equilibrium Bose-Einstein condensation, we strived to make a connection to particle production mechanisms as formulated in standard vacuum QFT. We conclude this thesis with a summary and a prospective outlook for further investigation.

Describing a phenomenon from a different framework requires one to be precise about the assumptions, the methods and language used in any attempt to uncover said phenomenon in terms of different degrees of freedom. To this end, this thesis was instigated in 1.2 with a comparison and distinction between the framework to-be-employed, the real-time Schwinger-Keldysh 2PI formulation of NeqQFT, and the asymptotic state formalism of vQFT. Since this thesis aimed to provide a first starting point towards considering Higgspllosion in a nonequilibrium framework, we subsequently introduced the conventional Higgspllosion formalism, its characteristics and consequences in 2.

Since we strived to describe processes of particle production, we attempted to discuss the advantages and remedies of an asymptotic particle picture by contrasting it to a dynamic and emergent particle picture in nonequilibrium theory in 3.1. Having had introduced the 2PI framework in 3.2, we reformulated the nonequilibrium 2PI equations of motion into a strong-field kinetic theory under the kinetic limit in 3.4, where a subsequent leading order strong-field coupling expansion to the 2PI effective action was employed. We arrived at a self-consistent scalar strong-field kinetic system of equations (3.84) including not only statistical and strong-field spectral dynamics, but also the dynamics of the background field itself. In contrast to ad-hoc zero-field kinetic theory employed for collider phenomenology or dark matter searches (for example [39]), our kinetic description emerges from the 2PI equations of motion solely by virtue of the kinetic limit such that a kinetic particle description is contained and uncovered for a sufficient reduction of complexity. Furthermore, the strong-field Boltzmann-like kinetic equation (3.84c) goes beyond semi-classical descriptions in that it also contains the background field dynamics as a participant of scattering processes in the form of an energy reservoir. This allows for more complex kinematics, where the background field can either fuel or impede an underlying process.

This closed kinetic system of strong-field equations is one of the main achievements of this thesis. Concisely presented in (3.84a), the background field equation of motion under the kinetic limit in the strong-field regime in conjunction with the spectral and statistical dynamics, (3.84b) and (3.84c) respectively, constitutes a self-consistent and coupled system of equations (3.84) for the complete dynamics of the system to LO in the strong-field coupling. Not ignoring the dynamics of the background field, this provides us with a novel approach to treating the kinetic dynamics of a strong-field system in order to study observables in their late-time evolution.

With a suitable kinetic description at our disposal, we ventured to isolate mechanisms of particle production in 3.5. We were able to identify two mechanisms explicitly. Both particle production mechanisms are driven explicitly by strong-field fluctuations. One mechanism is leading $\mathcal{O}(\lambda^0)$ in a strong-field coupling counting and encodes collisionless particle production through a drift term 3.5.1, where we made contact with a further mechanism for collisionless production of gap-less modes through an associated tachyonic instability. The other drives particle production through $\mathcal{O}(\lambda)$ inelastic scattering processes driven by strong-field fluctuations in the language of scattering amplitudes and decay rates 3.5.3. Isolating these mechanisms is another main achievement of this thesis.

Investigating collisionless particle production, the underlying mechanism driving $\mathcal{O}(\lambda^0)$ particle production (3.91) are the dynamics of the background field as encoded in the drift term (3.43). Through a discussion of the on-shell condition with respect to the strong-field spectral function (3.49), we were able to identify a further collisionless mechanism for the production of gap-less modes. Physically realized within a dynamical field-dependent momentum shell satisfying $|\vec{p}|^2 = -M^2[\Phi]$, the underlying behaviour is reminiscent of tachyonic instabilities as isolated in (3.97). Collisionless particle production as facilitated by the drift term does not directly rely on a coupling expansion. A counting in the coupling constant enters through the dynamics of the strong-field, which have to be solved for independently to given coupling order (3.84a). Explicitly solving for the dynamics of the background field will further provide insight into whether and how the strong-field regime $\Phi \sim 1/\lambda$ changes dynamically throughout time evolution. Exploring the collisional mechanism on the other hand, we were able to isolate a squared scattering amplitude (3.100) which is inherently local. In contrast to scattering objects in vQFT, it is not straightforward to define global scattering amplitudes for a process at hand since the explicit expressions very much dependent on the dynamics of the system. Asking whether a particle interaction will take place can only be answered for specific phase-space points, since the system dynamically evolves in time. Additionally, we were also able to identify a decay rate (3.110), which is again a local object and in its nature different from what one constructs in vQFT, compare (2.12). Provided a sufficient understanding of characteristic time scales of the system, one could recover global expressions through a time-averaging procedure. We have been able to identify the two rates at LO in the coupling, providing an intersection for the different frameworks. The agreement is remarkable, where an underlying reduction of the dynamical background field to a constant VEV is necessary and consistent with the reduction towards vQFT outlined in 1.2. What we observe again in this instance is that the possible kinematic processes in the nonequilibrium framework contain more channels of interaction to what is described in the framework of vQFT. As isolated in the $1 \rightarrow 2$ decay rate (3.110), particle production is directly encoded in the corresponding local scattering amplitude (3.100) and thereby driven by the dynamics of strong background field.

If one seeks to understand the process of Higgspllosion in particular, a translation between the vacuum and nonequilibrium framework is most likely in the language of scattering amplitudes. As we have seen for scattering amplitudes at NLO in the coupling in 3.5.2, one however has to consider a very high loop order for the emergence of

processes including a large final particle number. Such processes are therefore required to identify the nonequilibrium equivalent for the $1^* \rightarrow n$ amplitude (2.1) exhibiting the characteristic exponential growth behaviour in vacuum theory. Valuable insight is already contained in the $1 \rightarrow 2$ amplitude, which we recovered at LO (3.100), where a more in-depth understanding requires solving for the explicit dynamics of the background field in the context of the strong-field kinetic system (3.84) for suitable initial conditions. n point vertices at one-loop for strong-fields could also be isolated for the vacuum and nonequilibrium framework respectively through the Coleman-Weinberg potential.

Since certain phenomena of particle production can be understood through Bose-Einstein condensation, we concluded the application of our scalar kinetic system to particle production with a comparison to a conventional method of describing such a phenomenon within ad-hoc kinetic theory in 3.5.4. Identifying the condensate through the field in our framework and its dynamics through the corresponding strong-field equation (3.84a), our strong-field kinetic system is able to generalize the compared framework by separately describing statistical dynamics of the distribution function through a kinetic equation (3.84c) and the interaction with the condensate (3.116) through strong-field dynamics including additional source terms. Our strong-field kinetic system is therefore able to describe Bose-Einstein condensation self-consistently where the order parameter is identified to be $\Phi = \phi^2$.

We want to conclude this thesis by discussing the evolution of the strong-field scalar dynamics from initialization to thermalization as described within our framework.

Considering the strong-field regime, the field is initialized with a high amplitude from where it dynamically evolves towards and finally stabilizes in a minimum configuration. This evolution towards a minimum configuration results in particle production depleting energy from the initial strong field. This asymmetry towards field energy depletion and particle production is facilitated by the strong-field regime for small occupations since processes of particle annihilation into the field are suppressed. From another point of view, such an asymmetry of an effectively irreversible energy flow from the field towards the fluctuating modes is known to manifest itself through the process of dephasing corresponding to quantum decoherence of the off-diagonal elements of the initial Gaussian state [24]. After an initial phase of particle production through the initial field decay, the field starts to oscillate around a minimum configuration, where energy is transferred from the field through particle production or into the field through particle annihilation or decay processes. The partial dominance of processes scattering into the field becomes enhanced around a minimum configuration away from the strong-field regime, where an asymmetry however still remains and the oscillation remains effectively damped. Initially, particle production will therefore dominantly proceed through collisionless mechanisms such as the back-reaction through the effective mass facilitated by the initial strong fluctuations of the background field, or through instabilities 3.5.1. Approaching a minimum configuration, the oscillations of the field will transiently enhance either particle production from the field or particle annihilation into the field 3.5.3, where the field will either fuel or impede the respective processes. As we discussed in 3.3, taking the full nonequilibrium dynamics into account results in a wide range of

possible late-times values of the background field, where the final minimum configuration highly depends on the dynamics of the system at hand and how close to a possible minimum configuration the field was initialized to. Particle production could come to a transient halt if the field would get stuck in a meta-stable minimum through strong fluctuations resulting in a substantial deformation of the effective potential. Particles can not be produced from the field anymore after the field stabilized to its late-time thermalized value, which is facilitated by the collision terms in the kinetic equation (3.84c) and in the strong-field equation (3.84c) vanishing due to detailed balance as the particle distribution functions assume their thermal Bose-Einstein form.

Conventional kinetic theory is not able to describe early-time phenomena such as instabilities and small-scale interactions in the subsequent oscillatory evolution by virtue of assuming the late-time limit and a gradient expansion. Furthermore, kinetic theory employing an expansion in the coupling is not able to describe overoccupied systems, since higher-order diagrams are not necessarily suppressed¹⁴. Encompassing particle production reminiscent of tachyonic instabilities 3.5.1, Bose-Einstein condensation with a dynamical and consistent description of the order parameter $\Phi = \phi^2$ 3.5.4, a generalized treatment of scattering dynamics in a nonequilibrium setting 3.5.3 and a consistent treatment of strong-field dynamics (3.84a) however lends credibility to employing our kinetic system for the study of scalar phenomena up to the strong-field dynamics for moderately occupied systems.

From another point of view, the points of intersection between vacuum and nonequilibrium theory are a third main achievement of this work. We have found a means to reduce the multitude of degrees of freedom contained in a nonequilibrium description to isolate expressions established in vacuum theory. Exploring this intersection of two frameworks vastly different in information content allows one to find translations between the two. How the general reduction of complexity is achieved was already outlined in 1.2, we have however found explicit expressions such as nonequilibrium scattering amplitudes (3.100), which allowed us to further understand the thermalization process from a dynamical background field to a constant external vacuum expectation value in (3.103). To this end, understanding the reduction of information through thermalization allows one to understand a dynamical form of spontaneous symmetry breaking described in 3.3, which incorporates feedback effects and self-consistent dynamics in comparison to its conventional formulation 2.3.

Scrutinizing and further understanding this reduction of complexity towards textbook vacuum theory will allow us to further understand the process of thermalization, where a loss of sensitivity on the microscopic degrees of freedom and the emergence of macroscopic collective observables eventually leads to thermal equilibrium, which upon a subsequent zero-temperature limit and asymptotic construction is recast into the dynamics of vacuum correlators.

¹⁴From another point of view, the hierarchy between certain diagrams contributing to the evolution does not exist anymore such that a damped oscillatory behaviour towards a minimum configuration is not guaranteed

References

- [1] Valentin V. Khoze and Michael Spannowsky. "Higgspllosion: Solving the Hierarchy Problem via rapid decays of heavy states into multiple Higgs bosons". In: *Nuclear Physics B* 926 (2018). arXiv: 1704.03447.
- [2] Michael Peskin. "An Introduction To Quantum Field Theory, Student Economy Edition". en. CRC Press(2018).
- [3] Esteban A. Calzetta and Bei-Lok B. Hu. "Nonequilibrium Quantum Field Theory". Cambridge Monographs on Mathematical Physics. Cambridge University Press Cambridge (2008).
- [4] Sangyong Jeon. "Boltzmann equation in classical and quantum field theory". In: *Phys. Rev. C* 72.1 (2005). Publisher: American Physical Society.
- [5] Alex Kamenev. "Many-body theory of non-equilibrium systems". In: *arXiv:cond-mat/0412296* (2005). arXiv: cond-mat/0412296.
- [6] Kuang-chao Chou, Zhao-bin Su, Bai-lin Hao and Lu Yu. "Equilibrium and Nonequilibrium Formalisms Made Unified". en. In: *Phys.Rept.* 118 (1984).
- [7] Leonid V Keldysh. "Diagram technique for nonequilibrium processes". 20.4 (1965).
- [8] Julius Kuti. "The Higgs particle and the lattice". en. In: *PoS LATTICE2013* (2014).
- [9] Nima Arkani-Hamed, Tao Han, Michelangelo Mangano and Lian-Tao Wang. "Physics Opportunities of a 100 TeV Proton-Proton Collider". In: *Physics Reports* 652 (2016). arXiv: 1511.06495.
- [10] ALEGRO collaboration. "Towards an Advanced Linear International Collider". In: *arXiv:1901.10370 [physics]* (2019). arXiv: 1901.10370.
- [11] M. Carena, University of Chicago), C. Grojean (DESY, Hamburg, and Humboldt University, Berlin), M. Kado (Laboratoire de l'Accélérateur Linéaire, Orsay), and V. Sharma (University of, California, San Diego). and abdelhak Djouadi. "11. Status of Higgs Boson Physics".
- [12] M. V. Libanov, V. A. Rubakov, D. T. Son and S. V. Troitsky. "Exponentiation of multiparticle amplitudes in scalar theories". In: *Phys. Rev. D* 50.12 (1994). Publisher: American Physical Society.
- [13] M. B. Voloshin. "Loops with heavy particles in multi Higgs production amplitudes". In: *Phys. Rev. D* 95.11 (2017). arXiv: 1704.07320.
- [14] Valentin V. Khoze, Joey Reiness, Michael Spannowsky and Philip Waite. "Precision measurements for the Higgsploding Standard Model". In: *J. Phys. G: Nucl. Part. Phys.* 46.6 (2019). arXiv: 1709.08655.

- [15] Valentin V. Khoze and Michael Spannowsky. "The Higgsploding Universe". In: *Phys. Rev. D* 96.7 (2017). arXiv: 1707.01531.
- [16] Valentin V. Khoze, Joey Reiness, Jakub Scholtz and Michael Spannowsky. "A Higgsploding Theory of Dark Matter". In: *arXiv:1803.05441 [astro-ph, physics:hep-ph]* (2018). arXiv: 1803.05441.
- [17] Alexander Monin. "Inconsistencies of higgspllosion". In: *arXiv:1808.05810 [hep-ph, physics:hep-th, physics:math-ph]* (2018). arXiv: 1808.05810.
- [18] Valentin V. Khoze and Michael Spannowsky. "Consistency of Higgspllosion in Localizable QFT". In: *arXiv:1809.11141 [hep-ph, physics:hep-th]* (2018). arXiv: 1809.11141.
- [19] J. Berges, D. Gelfand and D. Sexty. "Amplified Fermion Production from Overpopulated Bose Fields". In: *Phys. Rev. D* 89.2 (2014). arXiv: 1308.2180.
- [20] Eliano Pessa. "The concept of particle in Quantum Field theory". In: *arXiv:0907.0178 [physics]* (2009). arXiv: 0907.0178.
- [21] J. Berges. "Introduction to Nonequilibrium Quantum Field Theory". In: *AIP Conference Proceedings* 739 (2004). arXiv: hep-ph/0409233.
- [22] J. Berges. "Nonequilibrium Quantum Fields: From Cold Atoms to Cosmology". In: *arXiv:1503.02907 [cond-mat, physics:hep-ph]* (2015). arXiv: 1503.02907.
- [23] G. Fauth. "Strong field QED kinetic equations from first principles". In: *Master thesis, University Heidelberg* (2019).
- [24] Fred Cooper, Salman Habib, Yuval Kluger and Emil Mottola. "Nonequilibrium dynamics of symmetry breaking in $\lambda\Phi^4$ theory". In: *Phys. Rev. D* 55.10 (1997). Publisher: American Physical Society.
- [25] Mathias Garny and Markus Michael Muller. "Kadanoff-Baym Equations with Non-Gaussian Initial Conditions: The Equilibrium Limit". In: *Phys. Rev. D* 80.8 (2009). arXiv: 0904.3600.
- [26] Iwo Bialynicki-Birula, Pawel Górnicki and Johann Rafelski. "Phase-space structure of the Dirac vacuum". In: *Phys. Rev. D* 44.6 (1991). Publisher: American Physical Society.
- [27] John M. Cornwall, R. Jackiw and E. Tomboulis. "Effective action for composite operators". In: *Phys. Rev. D* 10.8 (1974). Publisher: American Physical Society.
- [28] R. Walz, K. Boguslavski and J. Berges. "Large-N kinetic theory for highly occupied systems". In: *Phys. Rev. D* 97.11 (2018). arXiv: 1710.11146.
- [29] G. Fauth, J. Berges and A. Di Piazza. "Collisional strong-field QED transport and kinetic equations from first principles". In: *In preparation*.
- [30] Jürgen Berges and Benjamin Wallisch. "Nonthermal Fixed Points in Quantum Field Theory Beyond the Weak-Coupling Limit". In: *Phys. Rev. D* 95.3 (2017). arXiv: 1607.02160.
- [31] G. Aarts, D. Ahrensmeier, R. Baier, J. Berges and J. Serreau. "Far-from-equilibrium dynamics with broken symmetries from the 2PI-1/N expansion". In: *Phys. Rev. D* 66.4 (2002). arXiv: hep-ph/0201308.

- [32] Linda Shen, Jürgen Berges, Jan Pawłowski and Alexander Rothkopf. "Thermalization and dynamical spectral properties in the quark-meson model". In: *arXiv:2003.03270 [hep-ph]* (2020). arXiv: 2003.03270.
- [33] L.P. Kadanoff and G. Baym. "Quantum statistical mechanics: Green's function methods in equilibrium and nonequilibrium problems". Frontiers in physics. W.A. Benjamin(1962).
- [34] Gert Aarts and Jürgen Berges. "Nonequilibrium time evolution of the spectral function in quantum field theory". In: *Phys. Rev. D* 64.10 (2001). Publisher: American Physical Society.
- [35] S. Juchem, W. Cassing and C. Greiner. "Quantum dynamics and thermalization for out-of-equilibrium ϕ^4 – theory". In: *Phys. Rev. D* 69.2 (2004). arXiv: hep-ph/0307353.
- [36] N. V. Elkina, A. M. Fedotov, I. Yu Kostyukov, M. V. Legkov, N. B. Narozhny, E. N. Nerush and H. Ruhl. "QED cascades induced by circularly polarized laser fields". In: *Phys. Rev. ST Accel. Beams* 14.5 (2011). arXiv: 1010.4528.
- [37] Jean-Paul Blaizot and Edmond Iancu. "The quarkgluon plasma: collective dynamics and hard thermal loops". en. In: *Physics Reports* 359.5 (2002).
- [38] D. V. Semikoz and I. I. Tkachev. "Condensation of bosons in kinetic regime". In: *Phys. Rev. D* 55.2 (1997). arXiv: hep-ph/9507306.
- [39] Lawrence J. Hall, Karsten Jedamzik, John March-Russell and Stephen M. West. "Freeze-In Production of FIMP Dark Matter". In: *J. High Energ. Phys.* 2010.3 (2010). arXiv: 0911.1120.

4 Acknowledgements

First and foremost I would like to express my gratitude to Michael Spannowsky and Valya Khoze for providing me with the freedom and trust to explore the intersections between vacuum and nonequilibrium theory. Particularly grateful am I to Gregor Fauth, his thought-provoking comments, his guidance and our on-going discussions have helped me through and through to shape this project into what it has become and his intrinsic curiosity inspires me to this day to challenge my understanding of physics. Further, I want to thank Aleksander Chatrchyan and Kirill Boguslavsky for helpful discussions.

Statement of Authorship

I herewith declare that this thesis was solely composed by myself and that it constitutes my own work unless otherwise acknowledged in the text. I confirm that any quotes, arguments or concepts developed by another author and all sources of information are referenced throughout the thesis. This work has not been accepted in any previous application for a degree.

Durham, 8th September 2020

Chimo Preis